SeCURE
Saltwater intrusion and climate change: monitoring, countermeasures and informed governance

Deliverable 3.1.3 – Technical report on the investigation on climate change, its effect to low laying coastal agricultural areas in Croatian site and potential for the implementation to other vulnerable areas within the Adriatic basin
September 2023 – Final version

Contributing partners:
PP3 – UNIST, PP4 – DUNEA,
PP5 – PIDNIC

1. Contents

2. Introduction

The report has been thematically divided into two axes compiling the effort and the expertise of Croatian project partners and their specific contribution to the project objectives. In this way, specific attentiona has been given to the monitoring and analysis of Impact of saltwater intrusion on biodiversity (otter - Lutra lutra) in the Neretva Delta as a part of climate change impact to biodiversity. Additionally, specific attention has been given to the analysis of the processes controlling the seawater intrusion (SWI) along the Neretva Dekta with implications to mitigate negative climate change effects.

3. Impact of saltwater intrusion on biodiversity (otter - Lutra lutra) in the Neretva Delta

List of abbreviations and terms

ZZOP MZOE – Croatian Agency for the Environment and Nature, Ministry of Economy and Sustainable Development

HAOP – Croatian Environmental Protection Agency DZZP – State Institute for Nature Protection

Executive Summary

Eurasian otter (*Lutra lutra*) is a semiaquatic animal whose populations in Croatia have been declining for years. It's status according to the IUCN in Croatia is DD, i.e. Data

Deficient. In the area of Dubrovnik- Neretva County, there are two unconfirmed findings of otters in the vicinity of Lake Kuti. The aim of this research was to try to confirm the presence of otters in five special ornithological reserves of the Neretva river, which represent the largest remnants of Mediterranean reed beds in Croatia and are representative wetland ecosystems. Research was carried out by inspecting the study area for signs of presence and setting camera traps within the special ornithological reserves Kuti, Modro oko and Lake Desne, Orepak, Prud and Pod Gredom. After two field surveys and two months of recording with camera traps, not a single otter was recorded in the area of interest, and not a single sign of presence was recorded. Due to the marshland characteristics of the study area and the lush marsh vegetation, the method of investigating the presence of otter with camera traps is not recommended. Presence of otters in the area of special ornithological reserves should potentially first be confirmed using environmental DNA (eDNA) in order to reduce the research effort and conduct further targeted research and abundance estimation if the presence of otters is confirmed. The main reasons for endangerment are not the lack of quality habitats or salinization, but rather the anthropogenic influence that has changed over the last century from poaching to habitat degradation, canalization of watercourses and pollution of habitats that were once suitable for the otter and where it was once recorded. Anthropogenic pressure on protected areas is not easy to remove, therefore coordination of bodies in the service of environmental protection is needed in order to maintain and potentially increase the population of otter in the area of special ornithological reserves of the Neretva river.

A. Introduction

The company BIOTA d.o.o. conducted a field study of otters in the area of Dubrovnik-Neretva County within the special ornithological reserves of the Neretva river: Modro oko and Desne Lake, Pod Gredom, Orepak, Prud and Kuti.

Eurasian otter

Order: Carnivora Family: Mustelidae Genus: Lutra
Species: Eurasian otter (Lutra lutra L. 1785)

The otter is a semi-aquatic animal that can be recognized by its long slender body, short legs and long tail (Dobroruka, 2000). It can grow up to 135 cm and females are smaller than males which can weigh over 10 kg. The fur is brown to dark brown, with a lighter ventral side that is greyish to white. Some individuals can be distinguished by a lighter area in the form of a spot on the throat. When it is immersed in water its fur is smooth, while outside of water the fur dries quickly and the hairs stick together giving the animal a distinctive thorny appearance. Webbed digits can be found on all four legs (Jelić, 2010). The otter's diet is dominated by fish, crustaceans and amphibians (mainly frogs) (Parry et al., 2011). It has a well-developed sense of sight, hearing and sense of smell,

and only a small part of the communication between individuals takes place by means of recognizable vocalizations - piercing whistles, growls and beeps. Instead, they mark their territory with excrement which is called spraint and leave it on the paths they use, near places of entry and exit from the water and near resting places. Most of the spraints can be found on the most noticeable locations such as large rocks, tree trunks on the bank, under bridges or at confluences. In addition to droppings, anal jelly secretions are also common (Jelić, 2013; Dobroruka, 2000).

Ecology

Otters are most active at dusk when they hunt while spending the day in an underground den or in an above-ground shelter they build on quiet shores, usually sheltered by thick vegetation or old trees. Despite this, they can also be found in more open areas next to the roots of trees or on beds in marshy vegetation. Often the same individual uses a large number of places to rest (Jelić, 2013; Quaglietta et al., 2018). They are territorial animals, and several females can live within the territory of one male. It was believed that they are an extremely solitary species and associate only for mating. However, research has shown that otters are more social than previously thought, with adult males and females with cubs overlapping spatially and temporally and sharing diurnal resting sites more often than expected (Quaglietta et al., 2014). The gestation period is between 63 and 65 days and mating has been recorded throughout the year

(Dobroruka, 2000). Reproductive holts where the female gives birth to the cubs are further away from the stream, with inconspicuous entrances and are difficult to find because there are no spraints and visible tracks around them. The female raises 2-3 cubs which are blind for the first 35 days and enter the water for the first time at three months. At four months they learn to hunt independently, until then they are fed with their mother's milk. After about a year they become independent and while some stay close to the mother's territory, others can travel more than 150 km in search of their own territory (Jelić, 2010). In captivity they can live up to 17 years (Acharjyo and Mishra, 1983) while in nature they live much shorter, on average from 3 to 4 years (Jelić, 2010).

Habitat

They live in a wide variety of freshwater aquatic habitats, including highland and lowland lakes, rivers, streams, marshes and swamp forests, but they can also be found on seashores and in estuaries (Jelić, 2010; Beja, 1990). Research has shown that otters living near the coast use marine, freshwater and terrestrial habitats, but prefer to search for food in freshwater because inland prey is nutritionally more profitable. Also, by analyzing spraints it was determined that depending on the season the majority composition of marine/freshwater prey changes depending on its availability (Beja, 1991; Parry et al., 2011).

Otter signs of presence

The presence of an otter is generally relatively easy to research because it leaves numerous traces, i.e. signs of its presence. Otter spraint has a characteristic smell and appearance and is easily recognized by the fact that it contains fish scales and bones. There is fresh excrement, which is black-green in color, medium-old excrement (between one and three weeks old), which is dark and dry, and after three weeks it easily decomposes and turns gray (Jelić, 2013). Jelly secretions can be in various shades of brown and have an intense smell of fish oil. Footprints are also common and characteristic in appearance. The front foot has an almost round footprint between 6 - 6,5 cm long and is of lesser width. The hind foot is somewhat elongated and includes a heel tubercle and in some footprints claws and webbed skin can be seen (Jelić, 2013; Dobroruka, 2000).

Geographic range information

Of all Palearctic mammals, the otter has one of the largest ranges extending across Europe, Asia and Africa (Ando and Corbet 1966). After years of constant decline, the population is slowly recovering in Western Europe and the otter is now common in Austria, Bulgaria, the Czech Republic, Estonia, Hungary, Ireland, Latvia, Lithuania,

Montenegro, North Macedonia, Norway, Poland, Portugal, Slovakia, Spain, Sweden and the United Kingdom and is probably also common in Albania and Serbia. Population expansion in France, the Netherlands, Germany, Austria and Slovenia probably led to a reappearance in Switzerland, northern Italy and Belgium. However, otters are still extinct in Luxembourg, endangered in Italy, very rare in Switzerland and Belgium, and rare in western Germany and eastern France, and there is a lack of data to assess the situation in Belarus, Bosnia and Herzegovina and Kosovo (adapted from Loy et al., 2022).

In Croatia, the otter is widespread in the continental and highland water habitats, along the tributaries of the Drava, Danube, Sava, Kupa and Una, with rare exceptions such as the Kupa river upstream of Ozlje, the Dobra river upstream of Ogulin and the Gacka river. In the Mediterranean region, it is present in Lake Vrana and the rivers Zrmanja, Neretva and Krka and their tributaries. During the latest research, it was not recorded in Istria (Antolović et al., 2006; Jelić, 2010) (Figure 1). According to data obtained from the Ministry of Economy and Sustainable Development, there are two unverified findings of otters around Lake Kuti in the Dubrovnik-Neretva County. The first observation is from 2006, when spraints were found on the bridge in the village of Mlinište (Medunić-Orlić, 2007). The data from the second observation in 2009 is incomplete thus there is no definitive answer whether an individual was observed or only traces of its presence (Šijan, 2009). Relevant databases for the territory of Croatia such as iNaturalist, Biloger and Observation, were also reviewed. They are built on the

concept of collecting and mapping observations of biodiversity and consist of publicly available data collected by all interested individuals and all findings are validated with photographs. Not a single observation was recorded in the entire area of the Neretva river and the associated special reserves.

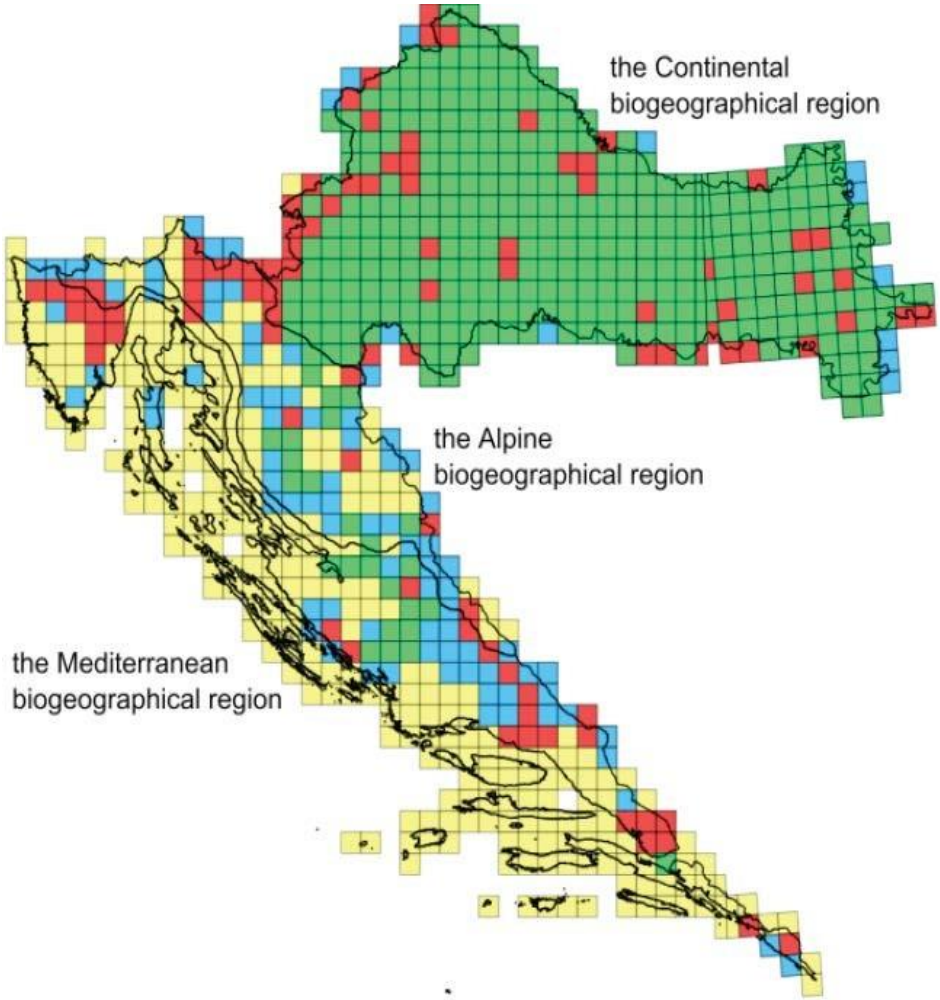

Figure 1 Otter distribution in Croatia (legend: green UTM fields 10 x 10 km - confirmed presence of otter;red fields - no otter findings; yellow fields - no suitable freshwater habitats; blue fields - nknown status)(adapted from Jelić, 2013)

Impact of saltwater intrusion

While researching otters, the properties of the water in which they live were also studied. The general conclusion was that within their natural values, the chemical properties of water indirectly affect otters through their impact on food supplies. An example is eutrophication which can have a positive effect if it leads to an increase in the number of fish while also a negative effect if it is excessive and achieves the opposite effect (Jelić, 2010). Although otters which live by the coast occasionally feed in the sea, it is extremely important that they have access to fresh water.

According to the research carried out in Scotland, it was noted that drying of sea water causes the formation of salt crystals on and in the inner layer of otter's fur. Larger mammals with fur that live or often swim in the sea have a thick layer of subcutaneous fat that helps maintain their body temperature. The otter, like most smaller semiaquatic mammals, uses its fur to maintain body temperature by retaining a layer of air inside the fur while swimming in water. Due to the formation of salt crystals, the otter's fur loses its water-repellency property and a significant drop in body temperature and visible tremors were observed in individuals that had access only to sea water for some time. Significantly longer cleaning and maintenance of fur after swimming through sea water was also observed. However, if fresh water is available near salt or brackish water, otters will use both habitats equally (Kruuk and Balharry, 1990).

Endangerment and protection status

The species is protected under the Nature Protection Act of the Republic of Croatia (Official Gazette 144/2013). It is also protected under a number of international legal and conservation statutes, including the Bern Convention (Appendix II), The European Union Habitats and Species Directive (Annex II and Annex IV) and The Washington convention - CITES (Appendix I). According to the IUCN Red List, globally and at the European level, the otter is Near Threatened (NT), while in Croatia it is considered as Data Deficient species (DD).

B. Study area

The study area consists of the special reserves of the Neretva river that surround it. Representative wetland ecosystems and diverse and developed wetland habitats can be found within five ornithological reserves (Modro oko and Lake Desne, Pod Gredom, Orepak, Prud and Kuti). On January 18th 1993. a large part of the Neretva Delta was included on the Ramsar list. Also, the entire course of the Neretva river from the border to the mouth of the river to the Adriatic Sea is part of the Natura 2000 POVS HR5000031 Neretva Delta, and the otter (Lutra lutra) is the target species of the area. The area of interest is covered with habitat type A.4.1 Reeds, sedges, tall sedges and tall sedges, and a very small part is combined with A.5.1. Orchards, A.2.4. Channels and I.1.8.

Neglected agricultural areas and I.2.1. Mosaics of cultivated areas (Bioportal, 2023).

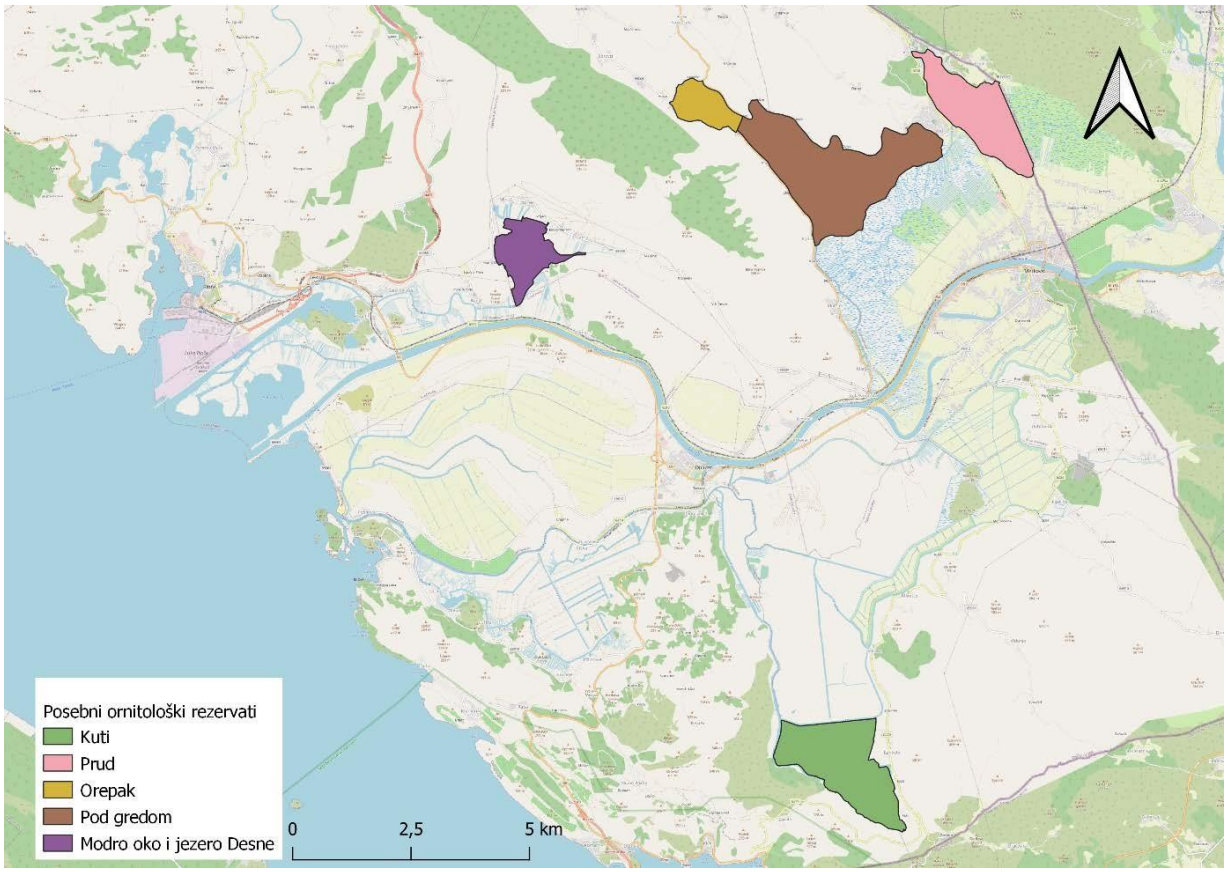

Figure 2 Study area

Modro oko and Lake Desne

Modro oko is a lake spring active all year round, located on the right bank of the Neretva

between Desna, Banja and Komin. It is part of a partially submerged karst depression and lies in a sinkhole at sea level. The deepest part is located at the center, which according to the latest research is at -23.1 m and is surrounded by steep slopes (Jelić, 2021). About 350 m long and 3.5 m wide canal is connecting it with Desne Lake, which has a similar configuration to Modro oko. Due to the white limestone of the sinkhole, the lake water is extremely blue in color. The waters of Modro oko and Desne are drained by the river Desanka and flow into Crna rika near the town of Banja, only 200 meters from the mouth of Crna rika into Neretva. Both lakes are supplied with water that comes from underground sources, but also from Neretva and its tributaries. That means they are under the influence of salty sea water (salinity ≤3), especially during the summer months when the water level of the Neretva is low. For this reason, the lake water is brackish to salty (ZZOP MZOE, 2020).

Modro oko and Lake Desne have been protected at the national level since 1974. as an important landscape. In order to preserve the habitat and diversity of wetland birds, the lake and the surrounding wetland area, the Croatian government passed the Decree on the Proclamation of Special Ornithological Reserves "Modro oko and Lake Desne", "Ušće Neretve" and "Kuti" (Official Gazette 94/2020). According to the aforementioned Decree, the significant landscape Modro oko and Lake Desne was reduced and recategorized into a special ornithological reserve, and now covers an area of 164.92 ha (ZZOP MZOE, 2020) (Figure 3).

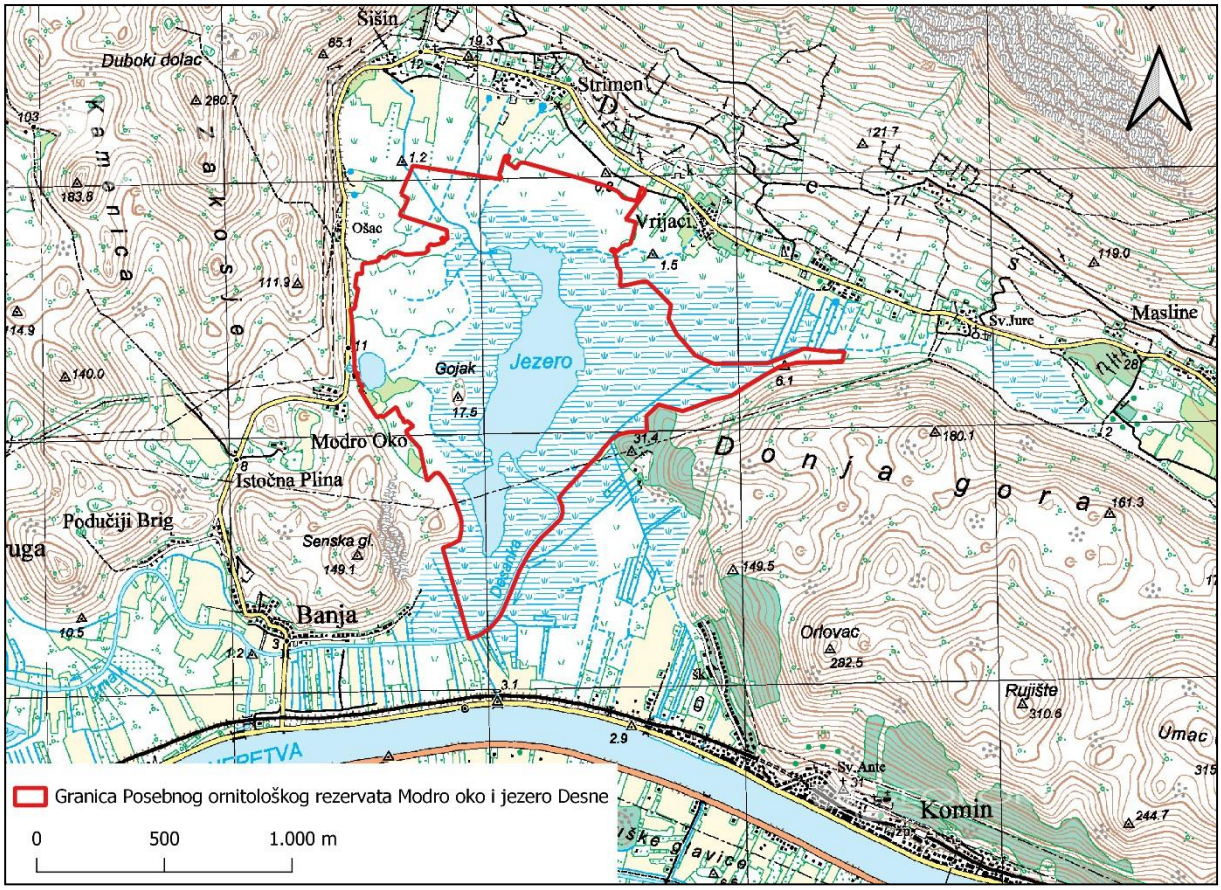

Figure 3 The border of the Special Ornithological Reserve Modro oko and Lake Desne

Pod Gredom, Orepak and Prud

The Special Ornithological Reserve Pod Gredom is a wetland area of the Neretva river near the town of Vid. It stretches to the east of the Matica river and to the north of the Norin river. The area is covered with reeds, rushes and other wetland plants. In the

vicinity of Norin river was reforested from 1968-1979. with autochthonous vegetation: willow, ash and poplar in order to attract bird species that seek groves and taller trees for nesting (e.g. herons) (HAOP, 2018). Part of the flooded river valley, with an area of 587 ha, was protected on March 17, 1965 as a special ornithological reserve due to its importance for nesting and migratory birds. After the GIS analysis, it officially covers an area of 551.50 ha (Bioportal, 2023).

The Special Ornithological Reserve Orepak is located near Vid, 5 km west of Metković and includes the valley around Gradina hill (HAOP, 2018). An area of about 100 ha was protected by the Decision of the Metković Municipality Assembly on October 7, 1974 due to its importance for migration and wintering of birds. After the GIS analysis, it officially covers an area of 96.91 ha. Orepak and Pod Gredom together form a biological whole (Bioportal, 2023).

The Special Ornithological Reserve Prud stretches east of Vid and Prud and north of Glibuša. The western side of the area is bounded by the river Norin, which springs within the protected area at the transition from the karst to the swampy area of the Neretva Delta. It represents an important natural science site where lush and interesting marsh vegetation stands out (HAOP, 2018). The surface of the Prud area, according to the protection act promulgated on March 17, 1965. is 250 ha, and after a GIS analysis it was determined that the area covers 261.13 ha (Bioportal, 2023).

Rezervati Orepak, Podgrede i Prud together represent the biggest remenants of

Mediterranean reed beds in Croatia (DZZP, 2009) (Figure 4).

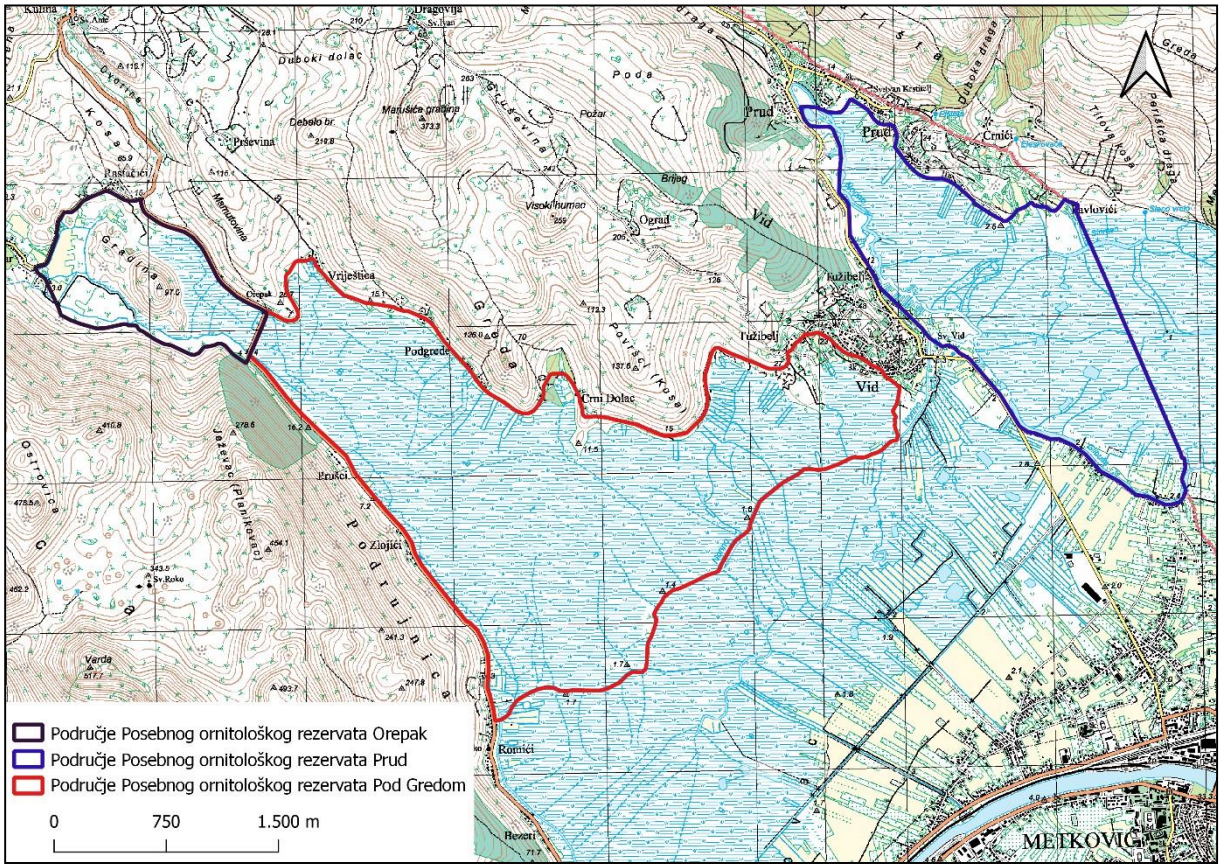

Figure 4 The borders of the special ornithological reserves Pod Gredom, Orepak i Prud

Kuti

Lake Kuti is an alluvial lake and crypto-depression located near the village of Bažula, 6 km south of the town of Opuzen, and combines a lake, swamp and karst landscape. It is supplied with water from several sources on the eastern and southern sides of the lake and flows north towards the Neretva with which it is connected by the Black River

and Mislin (ZZOP MZOE, 2020). Recent research has shown that there are two large underground springs within the lake which together with the large karst spring of Bažula probably provide the majority of the lake's water. Also, the greatest recorded depth was 4.6 m for a long time, however, with the discovery of a new spring and its depression, the new deepest part of Lake Kuti was determined at 17.4 m (Jelić, 2021). Despite the large amount of fresh water, a lower salinity of the lake was occasionally observed. Due to changes in the water level of the Adriatic Sea and changes in water pressure between fresh and sea water, there are frequent variations in the water level. During low water levels in the summer, an island appears in the northern central part of the lake (ZZOP MZOE, 2020).

Even though lake Kuti has diverse wetland habitats important for ornitofauna, the first time it received the status of a protected area was in 2020 when Croatian government passed the Decree on the Proclamation of Special Ornithological Reserves "Modro oko and Lake Desne", "Ušće Neretve" and "Kuti" (Official Gazette 94/2020). Since then Lake Kuti is under protection and covers an area of 338.86 ha (ZZOP MZOE, 2020; Bioportal, 2023) (Figure 5).

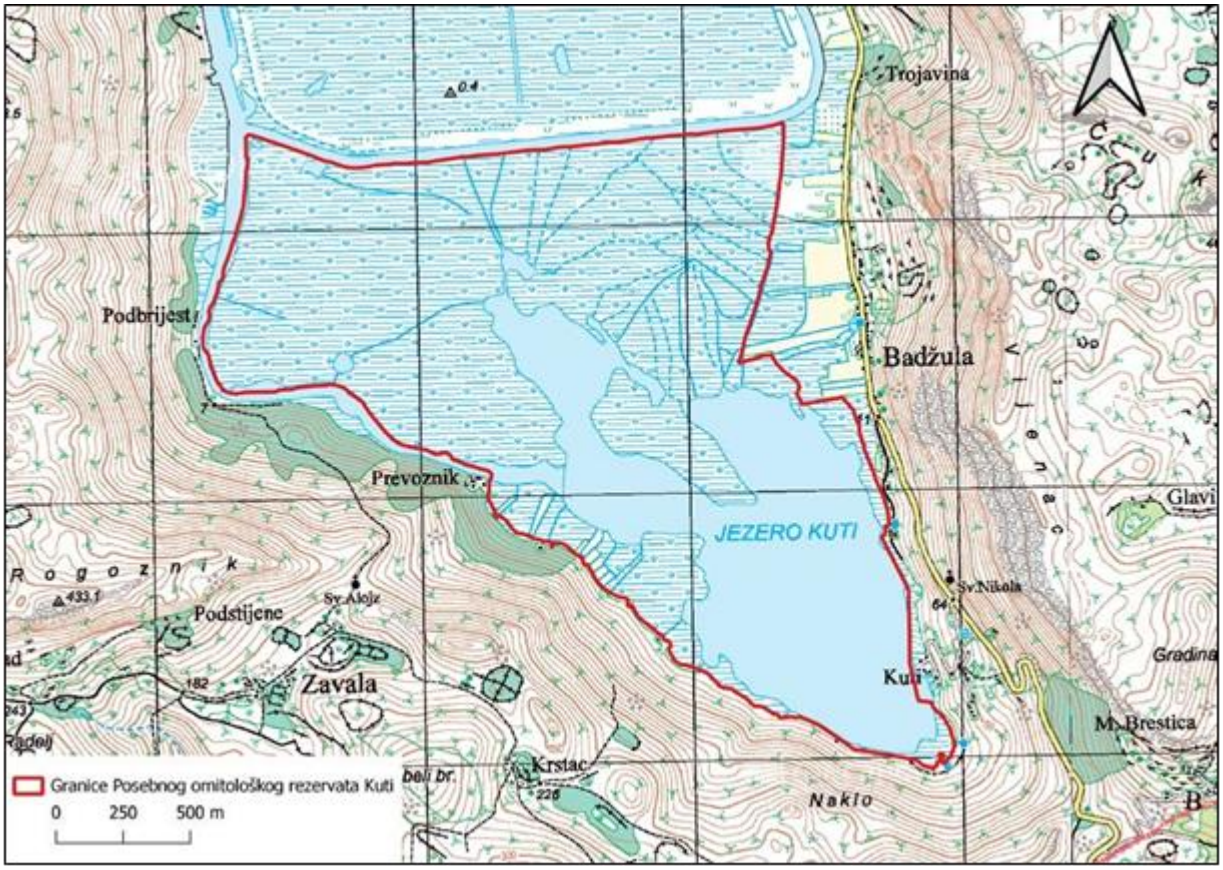

Figure 5 The border of the Special Ornithological Reserve Kuti

C. Research objectives

1. Overview of previous research and available literature data on otters in the Dubrovnik-Neretva County with an emphasis on special reserves of the Neretva river (i.e. the vicinity of Natura 2000 POVS HR5000031 Neretva Delta);

2. Field research with the aim of determining the presence of otters in special reserves of the Neretva (i.e. the surroundings of the Natura 2000 POVS HR5000031 Neretva Delta);

3. Processing of the collected data and preparation of the Report on the presence of otters in special reserves of the Neretva (i.e. the surroundings of Natura 2000 POVS HR5000031 Neretva Delta).

D. Methodology

Field research within special reserves of the Neretva (i.e. the surroundings of Natura 2000 area HR5000031 Neretva Delta) is planned from the beginning of April to the end of May 2023. The research includes a non-invasive method of monitoring using camera traps and recording signs of presence by searching the terrain with the aim of confirming the presence of otter in the area of interest.

Camera traps

The great advantage of camera traps is that they can collect high-quality and numerous data without the long-term presence of researchers in the field and without disturbing the animals. The data can also be reviewed by other experts. Denver WCT-8010 photo

traps were used for recording wild animals with video resolution 1440 x 1080 pixels and photo resolution 8 megapixels. The camera traps are set to take a photo first followed by a 10 seconds long video. 1-minute interval between shots is set so that the same individual does not activate the camera trap again in a short period of time. The sensitivity of the motion sensor is set to medium. All findings (camera traps, tracks) were recorded using a Garmin GPS device or the software application OruxMaps v.7.4.23 in the WGS 84 coordinate system. They were later processed in the software QGIS v3.22.6 and transformed into the HTRS coordinate system.

Camera traps were placed at 10 locations within the Neretva special reserves. Four camera traps were placed in the area of the Special Ornithological Reserve Kuti, two camera traps each were placed in the areas of the Modro oko and Jezero Desne and Pod Gredom special ornithological reserves, and one camera trap was placed in the areas of Orepak and Prud special ornithological reserves. Locations for camera traps are usually selected by comparing the available data, in this case on otter presence, and suitable habitats within research area. Considering that all findings were outside of reserves boundaries, watercourses within were designated as best suitable habitats. Loacations should be inconspicuous to passers-by (hunters, foresters, residents, etc.) but in areas where otter activity is visible (presence of prints, feeding traces, spraints, jelly secretions) and places of potential movement and retention.

However, research area is very inaccessible with very few access points. No signs of otter presence were found, therefore the locations for camera traps were chosen on

the spot by following criteria: immediate proximity to watercourses; potential marking sites along the coast with larger stones or prominent elements that are not washed away by water and can be marked by the otter; present coastal vegetation on which it is possible to place a camera trap; with as little as possible aquatic vegetation so that the camera trap is not activated by the wind; as secluded as possible so that the camera trap does not get stolen and thus valuable data lost (Figure 6). That is why some camera traps were set up slightly outside the borders of special ornithological reserves, but on watercourses that are closely connected with them. If the presence of otters is confirmed at any of these locations, it can be safely said that they also live in the special ornithological reserves (Figure 7, Table 1).

Figure 6 A camera trap placed in the Special Ornithological Reserve Orepak

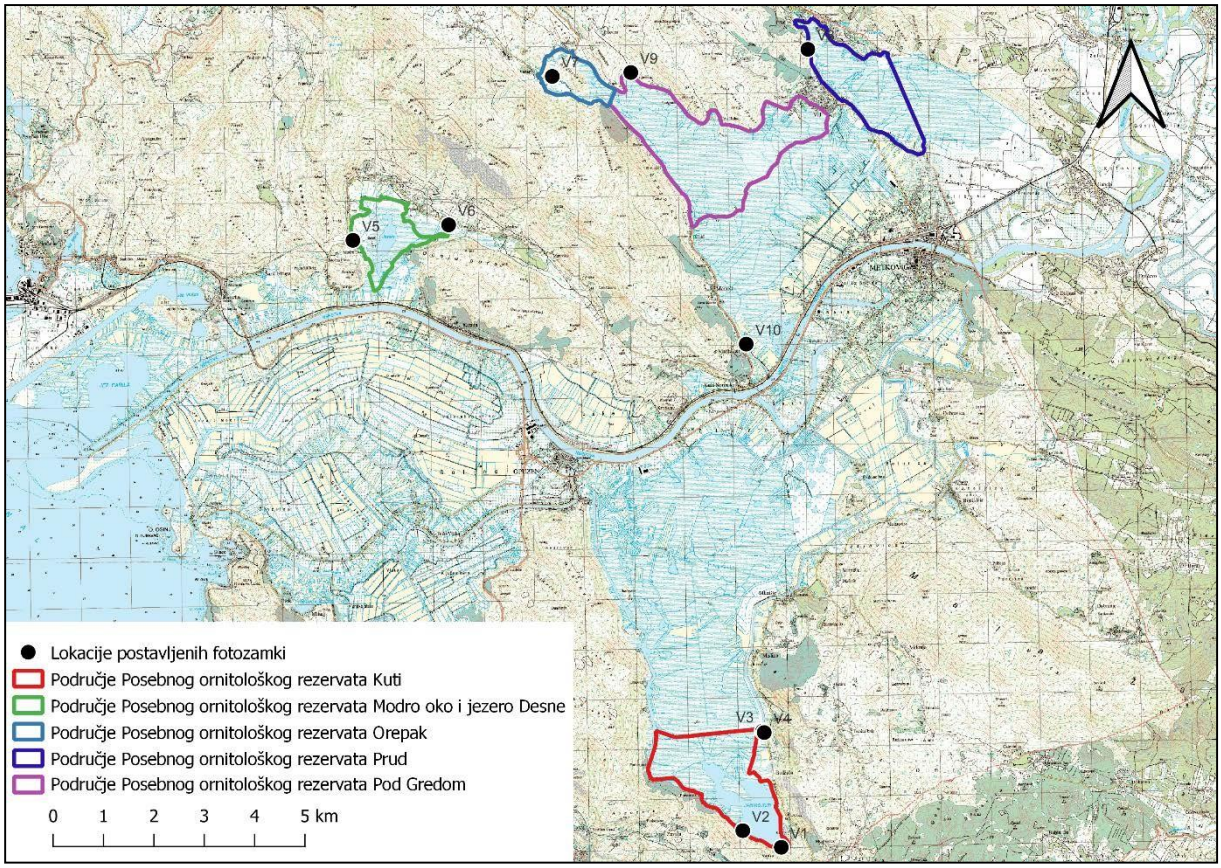

Figure 7 Locations of camera traps

Table 1 Coordinates of camera traps placed within special ornithological reserves of the Neretva

Camera trap	X	Y	Locality
V1	590811,1	4757038,2	Kuti, south
V2	590046,3	4757368,4	Kuti, southwest (Čovića vir)
V3	590439,1	4759343,5	Kuti, agro ethno park Žabac
V4	590472,4	4759317,9	Kuti, agro ethno park Žabac
V5	582305,3	4769094,9	Modro oko
V6	584205,9	4769402,4	Lake Desne canal
V7	586263,5	4772351,9	Orepak, unnamed stream

V8	591338,0	4772889,4	Prud, on the Norin river
V9	587823,3	4772428,9	Pod Gredom, spring near Vriještica
V10	590114,5	4767033,8	Pod Gredom,on the Norin river

Field survey

Field surveys should be done according to the Croatian National Monitoring Plan made specifically for otter. The standard method uses surveys of stretches of 600 m of river banks for searching evidence of otter presence. Starting points are usually bridges because they provide access to the water and enable the selection of the coast along which to work. Bridges are also the most suitable places to confirm the presence of otter because in sheltered places the spraints can persist for up to twelve months (Jelić, 2013). However, in wetlands like this it is not possible to conduct field surveys this way. Due to lush vegetation and mud, walking along the coast is not possible. Suitable areas for searching are mainly along the canals that are located next to private, mostly fenced arable land. Everything outside private agricultural lands is overgrown with thick maquis and sedge.

Therefore, surveying lake and river banks for searching evidence of otter presence was carried out opportunistically during two fieldworks, a total of five days.

E. Results

A total of 10 camera traps were placed within (and near) five special ornithological reserves of the Neretva river. The camera traps were set in the period from April 3 to 5, 2023, left to record continuously, and collected on June 1 and 2, 2023.

During this period, the camera traps were active for 152 days. Active days are calculated by adding up all the days when the camera traps were in operation, regardless of whether they recorded something every day. The days when the camera shuts down, either due to empty batteries, a malfunction or a full card are not counted. An event is defined as all activity of same species recorded within a certain period of time. Generally, a range between 10 and 60 minutes is taken depending on the observed species (Meek et al., 2014). During analysis of the obtained data one event was defined as a period of 10 minutes (Table 2).

Table 2 – Camera trap activity

Number of locations	Active days	Number of events	Animal count	Average number of events recorded per camera per day
10	152	220	294	0,70

During two months of monitoring a total of 7,585 shots were recorded, of which 4,246 photos and 3,339 videos. Birds were the most represented animal class with 288 recordings in a 204 events, 28 people were recorded in 16 events and also one rodent

and two bats.There are also three recordings where it was not possible to identify the animal even to the class level. This results were expected considering that the research was carried out within special ornithological reserves. Unfortunately, not a single otter was recorded in any of special ornithological reserves of the Neretva as well as a single sign of otter presence.

During the field surveys we spoke with local residents who claim that the otter used to be present in all watercourses in the area, but that they have not seen it in a long time. Only one gentleman who lives right next to Lake Kuti stated that he has continuously seen the same damages in the kiddles for years which he attributes to the otter, but he also claims that there used to be much more of them.

It is important to note that the reason for such a small number of active camera trap days lies in the combination of demanding terrain and a method that is not the best fit for wetlands. Although camera traps generally are used successfully as a method for otter research, there is a big difference in the type of habitat within the research is carried out. The main premise of camera traps is that they are in a sleep mode until something activates them, be it an animal or some other factor such as wind, sun, shadow. For this reason clean locations are needed, without a lot of vegetation that could often trigger the camera trap. The areas of the special reserves are wetlands where it was not possible to clear all the vegetation that could potentially activate the camera trap. Also, the camera traps face the water surface, which means that any ripple

in the water or movement of the vegetation reflected in the still water could have activated them.

Saltwater intrusion

Water salinity was not measured while conducting this field research. However, a detailed literature review was done. According to Croatian Agency for the Environment and Nature (2020) on lake Kuti were occasionally observed lower saltwater intrusions while for Modro oko and lake Desne it is stated that water is brackish to saline. Given that there was no continuous monitoring of the physico-chemical parameters of the water for the last 10 years, it is not possible to determine the impact of saltwater intrusion on special ornithological reserves with certainty, but according to several different researches conducted over a number of years, it has been shown that Modro oko is under the greatest influence.

All special ornithological reserves are connected by tributaries to the main course of the Neretva River, which is connected to the sea through its delta. There is halocline present in the Neretva river almost all year round which, depending on the season reaches up to 25 km from the confluence. However, during high flows the salt wedge is completely withdrawn from the river bed. Therefore, the saltwater intrusion depends mostly on the amount of fresh water that comes through the tributaries and the flow

rate of the Neretva. It is important to note that even with minimal flow, fresh water always flows in the surface layer (Ljubenkov and Vraneš, 2012). This means that the salinity of lakes Modro oko, Desne and Kuti and of the Norin river, which flows through Prud and Pod Gredom, also varies depending on the season.

The diatoms were studied in lakes Modro oko, Desne and Kuti throughout the seasons in 1994, 1995, 1997, and 1998 and continuous measurements of salinity were made at different depths. There was no salinity difference observed between shallow and deep samples. The highest salinity recorded was in Modro oko with a maximum value of 2.5 ‰, while it was stated that seawater has no influence on lake Kuti (Jasprica and Hafner, 2005; Jasprica 2007). During a one-year study of the microscopic crustaceans in lake Kuti, salinity was measured on a monthly basis from June 2012 to May 2013. A slight increase in salinity from 0.1‰ to 1.1‰ was recorded during that period (Planinić, 2017). Also, while mapping lakes Modro oko and Kuti, it was determined by diving that there is no clear boundary between fresh and salt water, i.e. no halocline is present (Jelić, 2021). It is possible that due to the nature of the underground sources that fill the lakes and the extremely dynamic flow of water, there is no stratification of the layers. The spring water and the water from the tributaries are mixed with each other, so for this reason vertical salinity variations are not expressed (Jasprica and Hafner, 2005). Through the research conducted in the area of the Prud spring which is the source of the river Norin, from March 2014 to November 2015, a slight increase in salinity was also determined during the summer period with a maximum recorded value of 0.41 ‰ (Šunjić, 2016).

F. Conclusions

1) In two months of continuous monitoring at 10 locations within the special ornithological reserves of the Neretva River, no otter or signs of its presence were recorded, although the habitat itself is suitable for this species. As a result of the analysis of the available data on the salinity of the researched area, it can be concluded that the special ornithological reserves are not greatly influenced by salinity and that this is not the key reason for the absence of the species from the area of interest.

2) Considering the characteristics of the researched area the camera traps are not the best method of otter detection. For further research of this species we would suggest the environmental DNA (eDNA) method. Confirmation of the presence of otters within each of the areas of interest could be obtained from filtered water sampled within the special ornithological reserves. This way, the research effort would be reduced and monitoring of the condition, distribution and especially abundance could be done in targeted areas. Surveying lake and river banks within ornithological reserves is almost impossible due to the large amount of mud and aquatic vegetation. Instead of a transect along the coast, it would be much easier to do it by boat along the coast. It should also be noted that the optimal months for otter research are during the coldest part of the year, from November to February. Due to the lesser presence of vegetation, it is much easier to see the traces that remain untouched for the longest

period of time.

3) The main reasons for the endangerement are anthropogenic in nature, the presence of cities in combination with very pronounced agriculture which cause habitat degradation. Aquatic habitats are particularly sensitive to human-caused changes. Channelization of rivers, removal of riparian vegetation, construction of dams, wetlands drainage and related human-made impacts are unfavorable to otter populations (Reuther and Hilton-Taylor, 2004). Pollution is a major threat, especially organic pollution with nitrate fertilizers and untreated wastewater as it results in acidification of rivers and lakes which causes a decrease in fish biomass (Loy et al., 2022). In the Neretva delta, discarded and forgotten nets and kiddles together with poachers pose a great danger. Only 8 km upstream, at the confluence of the Trebižat river in Neretva, members of a fishing society found three dead otters in a net of poachers which shows just how dangerous nets and kiddles are (Matić, 2010).

4) The main aspect of otter protection is the reduction of anthropogenic impact. Potential protection measures require good coordination of all institutions in the service of nature protection because anthropogenic threats are not unambiguous. The same institution is not responsible for monitoring illegal construction, channeling watercourses or conducting control of farmers, etc. It is necessary to ensure better compliance with existing laws and stop further habitat degradation in the whole Neretva Delta. Solid waste and abandoned fishing tools can be removed in cooperation

with local hunters, fishermen and volunteers through organized clean-up actions.

G. Literature

Acharjyo, L.N., Mishra., C.G. (1983): A note on the longevity of two species of Indian otters in captivity. Journal of the Bombay Natural History Society 80(3): 636.

Ando, M., Corbet, G.B. (1966): The Terrestrial Mammals of Western Europe. G.T. Foulis & Co., London, UK.

Antolović, J., Frković, A., Grubešić, M., Holcer, D., Vuković, M., Flajšman, E., Grgurev, M., Hamidović, D., Pavlinić, I., Tvrtković, N. (2006): Crvena knjiga sisavaca Hrvatske. Ministarstvo kulture, Državni zavod za zaštitu prirode, Zagreb.

Beja, P.R. (1991): Diet of otters (Lutra lutra) in closely associated freshwater, brackish, and marine habitats in south-west Portugal. Journal of Zoology (London) 225: 141-152.

Biologer - https://biologer.hr/hr, pristupljeno 19.06.2023.

Dobroruka, L. J. (2000): A field guide in colour to mammals. Silverdale Books, Bookmark Ltd., Leicester.

DZZP (2009): Prirodoslovna podloga za Izmjene i dopune Prostornog plana Dubrovačko- neretvanske županije.

HAOP (2018): Pregled i procjena usluga ekosustava na tršćacima Republike Hrvatske. iNaturalist - https://www.inaturalist.org/, pristupljeno 19.06.2023.
Jasprica, N. i Hafner, D. (2005): Taxonomic composition and seasonality of diatoms in three Dinaric karstic lakes in Croatia. Limnologica 35 (2005) 304-319.

Jasprica, N. (2007): Flora delte Neretve. Biljni svijet u delti Neretve. Regionalni centar zaštite okoliša za Srednju i Istočnu Europu. 34.

Jelić, M. (2010): Vidra - Priručnik za invertarizaciju i praćenje stanja (the Otter - manual for inventarisation and monitoring). DZZP, Zagreb.

Jelić, M. (2013): Nacionalni programi za praćenje stanja očuvanosti vrsta - Vidra (Lutra lutra). DZZP, Zagreb.

Jelić, D. (2021): Mapping of transitional habitats and biodiversity in lake Kuti and Modro oko. Izvještaj, BIOTA d.o.o.

Kruuk, H., Balharry, D. (1990): Effects of sea water on thermal insulation of the otter,

Lutra lutra. Institute of Terrestrial Ecology, Banachory, Scotland. J. Zool., Lond. (1990) 220, 405-415.

Loy, A., Kranz, A., Oleynikov, A., Roos, A., Savage, M., Duplaix, N. (2022): Lutra lutra (amended version of 2021 assessment). The IUCN Red List of Threatened Species 2022: e.T12419A218069689. Pristupljeno 08.06.2023.

Ljubenkov I. i Vranješ, M. (2012): Numerički model uslojenog tečenja – primjer zaslanjivanja korita rijeke Neretve (2004.) Građevinar 64 (2012) 2, 101-112.

Matić, F. (2010): Na ušću Trebižata u Neretvu u mreži krivolovaca pronađene tri uginule vidre, Bistro Bosno i Hercegovino! - http://www.bistrobih.ba/nova/2010/10/22/na-uscu-trebizata-u-neretvu-u- mrezi-krivolovaca-pronadene-tri-uginule-vidre/, objavljeno 22.10.2010., pristupljeno 19.06.2023.

Meek, P. D., Ballard, G., Claridge, A., Kays, R., Moseby, K., O'brien, T., O'Connell, A.,

Sanderson, J., Swann, D.E., Tobler, M., Townsend, S. (2014). Recommended guiding principles for reporting on camera trapping research. Biodiversity and conservation, 23(9), 2321-2343.

Medunić-Orlić, G., Šijan, M., Carev, I. (2007): Rezultati terenskih istraživanja u okviru

projekta „Istraživanje vidre (Lutra lutra L.) u Dalmaciji“ Udruge Sunce.

Observation.org - https://observation.org/, pristupljeno 19.06.2023.

Parry, G., Burton, S., Cox, B., Forman, D. (2011): Diet of coastal foraging Eurasian otters (Lutra lutra L.) in Pembrokeshire south-west Wales. European Journal of Wildlife Research. 57. 485-494. 10.1007/s10344-010-0457-y.

Planinić, A. (2017): Faunistička i ekološka karakterizacija zajednica mikroskopskih rakova (Copepoda i Cladocera) u jezerskim i izvorskim staništima donjeg toka rijeke Neretve. Doktorski rad. Zagreb: Sveučilište u Zagrebu, Prirodoslovno-matematički fakultet.

Quaglietta, L., Mira, A., Boitani, L. (2018): Extrinsic and intrinsic factors affecting the daily rhythms of a semiaquatic carnivore in a Mediterranean environment. Hystrix, the Italian Journal of Mammalogy 29(1): 128-136.

Quaglietta, L., Fonseca, V.C., Mira, A., Boitani, L. (2014): Sociospatial organization of a solitary carnivore, the Eurasian otter (Lutra lutra). J. Mammal. 95: 140–150.

Reuther, C., Hilton-Taylor, C. (2004): Lutra lutra. 2007 IUCN Red List of Threatened Species. IUCN 2007.

Šijan, M. (2009): Znanstvena analiza euroazijske vidre (Lutra lutra L.) s dodatka II i IV direktive o zaštiti prirodnih staništa i divlje faune i flore na području mediteranske i alpske biogeografske zone hrvatske. Udruga Sunce.

Šunjić, P. (2016): Zajednica vodenih beskralješnjaka izvora Prud u delti Neretve. Diplomski rad. Zagreb: Sveučilište u Zagrebu, Prirodoslovno- matematički fakultet.

Zavod za zaštitu okoliša i prirode Ministarstva gospodarstva i održivog razvoja (2019): Bioportal. Dostupno na http://www.bioportal.hr/. Pristupljeno: 08.06.2023.

ZZOP MZOE (2020): Stručna podloga za izmjenu granica Posebnog ihtiološko-ornitološkog rezervata jugoistočni dio Delte Neretve, izmjenu granica i prekategorizaciju Značajnog krajobraza Modro oko i jezero uz naselje Desne te zaštitu područja Kuti u kategoriji posebnog ornitološkog rezervata - II. izmjene

4. Response of the groundwater system to external loadings induced by limate changes

A. Introduction

Coastal aquifers worldwide are negatively affected by seawater intrusion (SWI)

(Custodio, 2010; Mastrocicco and Colombani, 2021; Werner et al., 2013) which is reflected through the changes in groundwater quality and reduced crop productivity in agricultural areas. These changes are expected to increase significantly as the climate changes progress (Da et al., 2015; Ketabchi et al., 2016; Oude Essink et al., 2010; Racetin et al., 2020; Sithara et al., 2020).

Besides SWI, salinization of coastal aquifers can be caused by anthropogenic contamination (de Oliveira Gomes et al., 2019; Saidi et al., 2009), rock-water interactions (Kharroubi et al., 2012; Najib et al., 2017; Rosenthal et al., 2007) and from by the flow of saline water from underlying adjacent aquifers upwards (Rosenthal et al., 2007). Coastal aquifers can be also salinized due to the presence of palaeo-seawater (Delsman et al., 2014; Shi and Jiao, 2014). Following the origin evolution of coastal aquifers from the Holocene to the present, older groundwater is typically found in lower coastal subaquifers (Yechieli and Sivan, 2011). Consequently, palaeo-seawater intrusion typically occurs through the uprising of lower subaquifers into subaquifers closer to the ground surface (Re and Zuppi, 2011). However, depending on the hydrogeologic evolution of study area, sources of palaeo-seawater can also be found in the shallow aquifers (Carol et al., 2021; Vallejos et al., 2018). Standard techniques for identifying sources of salinity in coastal aquifers rely on determining the relationship between major ions (Santucci et al., 2016). However, ion ratios cannot solely be used to successfully identify palaeo-seawater intrusion (Frollini et al., 2022). Consequently, the analysis of environmental isotopes can be used to identify both palaeo-seawater and modern seawater due to the isotopic fingerprint that distinguishes these distinct

sources of the salinity (Argamasilla et al., 2017). Due to the fact previously mentioned methods require sampling of surface water and groundwater and laboratory analysis of these samples to determine changes at the time scale characterizing the area of interest in groundwater, it is necessary to continuously monitor groundwater parameters and analyse datasets obtained through the monitoring system-obtained datasets.

Throughout historyUp to date, various approaches emerged to understand the transient nature of SWI. The impact of SWI can be predicted fairly accurate by using dual-density numerical models and laboratory experiments (Kuan et al., 2019; Levanon et al., 2019; Paldor et al., 2019; Stein et al., 2019; van Engelen et al., 2019; Xu et al., 2019). Geochemical analysis has been proven as a successful tool for identifying salinization processes in coastal areas (Behera et al., 2019; de Oliveira Gomes et al., 2019; Khan et al., 2020; Najib et al., 2017). In addition to the aforementioned approaches, time series analysis of data obtained from installed monitoring systems in coastal aquifers has been provend to be an efficient approach for determining hydrogeological parameters (Fuentes-Arreazola et al., 2018; Xia and Li, 2009) and identifying SWI processes and salinity regimes of the groundwater as found within the coastal aquifer systems (Vallejos et al., 2014; Wood and Harrington, 2015; Yang et al., 2020; Zhang et al., 2020). SWI as found at specific coastal systems have been a research subject of multiple number of research groups during the ongoing decade. Numerical modelling approach has been used in the work by (Dibaj et al., 2021) to investigate the peculiarities affecting

SWI in Taiwan site. Australian national inventory of SWI has been elaborated within the work by (Morgan and Werner, 2015). Dual-density modelling has been shown as a useful tool for water management on of coastal systems (Abd-Elaty and Zelenakova, 2022). This is especially a helpful during SWI risk assessment analysis due to caused by the climate change projections. In a similar manner, zoning of coastal aquifer area based on TDS, salinity and geochemical features have has been presented in (Vahidipour et al., 2021).

The Kimje coastal area in Korea has been the subject of research by (Kim et al., 2005), where the relationship between observed time series of seawater elevation (SWL) and groundwater level (GWL) versus electrical conductivity (EC) in piezometers has been established, leading to the conclusion that the groundwater quality is subjected to tidal in fluencees. A sSimilar methodology was has been used to show demonstrate that tides affect the movement of the saltwater-freshwater interface in Jeju Island, Korea (Kim et al., 2006). Jeju Island has been was again the subject of a research by (Kim et al., 2008a), who analysed the dynamic behaviour of saltwater-freshwater interaction at five different coastal zones. The resultsResults showed that GWL, EC and temperature (T) were have been affected by tidal variations and intensive precipitation. Monitoring systems once again have been provend as a tool with a capacity to capture for relevant information along the Venice coast in Italy, where SWI vulnerability has been assessed by taking into account EC, GWL and distance to saline and freshwater sources (Da et al., 2015). Lovrinović et al., (2021) investigated the capacity of two independent monitoring systems, one in Neretva Valley and the second in the Venice Lagoon in Italy, based on

observed GWL, EC and T time series. Both monitoring systems were have been found to be capable of capturingto offer necessary information for the identification of SWI processes.

Neretva Valley represents the largest agricultural area in the coastal area of Croatia. Conservation of the area means long-term sustainability of the population living in the valley, which further emphasises the need for the monitoring and understanding the transient nature of SWI present hereby. Previous studies in Neretva Valley were have been conducted as a pre-project phases for water management infrastructure implementation. Hydrogeological characterization of Neretva Valley has been performed in the study of (Srzić et al., 2020) while several studies dealt with SWI related problems in Neretva coastal system (Lovrinović et al., 2022, 2021; Racetin et al., 2020; Romić et al., 2020; Zovko et al., 2018).

B. Study area

Historical overview and geographical settings

River Neretva Valley is located in the very southeastern part of Croatia (Figure 1.). Specific part of the valley located between the Adriatic Sea to the west and town Opuzen to the east, called Neretva valley has been considered as an area of interest of this paper. Through the 20th century, the alluvial soil of the Lower Neretva valley has been identified as a highly potential agricultural area mainly by local population. Until the

second half of 20th century, most of 4200 ha of the Neretva valley was mainly a marshland. Starting from 1960s up to date, an infrastructural development led to the construction of embankment Diga creating a physical barrier between the study area and the Adriatic Sea (Figure 1), melioration channels and pumping stations. With the implementation of, firstly melioration and later flood protection and partially irrigation systems, better agricultural conditions have been reached and kept up to date.

Study area is alluvial delta fed by the alluvium from river Neretva. It is surrounded by karstic hills to the north as well as to the south and southwest. Terrain elevation of the valley's central part ranges between -2,50 to 2,00 m a.s.l. "Nula Trsta" vertical datum is used as reference for all elevation data along the paper as well for absolute piezometric head values used within the paper. While the embankment Diga (Figure 1) is recognised as a border between Adriatic Sea and the inland to the west, river Neretva represents a natural boundary to the north while Mala Neretva mimics the border of the Opuzen usce area to the south. Opuzen usce area can be divided into two specific sub areas, respectively Jasenska and Crepina as seen in Figure 1. Vidrice area is separated melioration subsystem located to the south from river Mala Neretva and is surrounded by karstic hills to the east, south and west. Along the Vidrice area, the terrain elevation ranges between -1,50 to 1,00 m a.s.l..

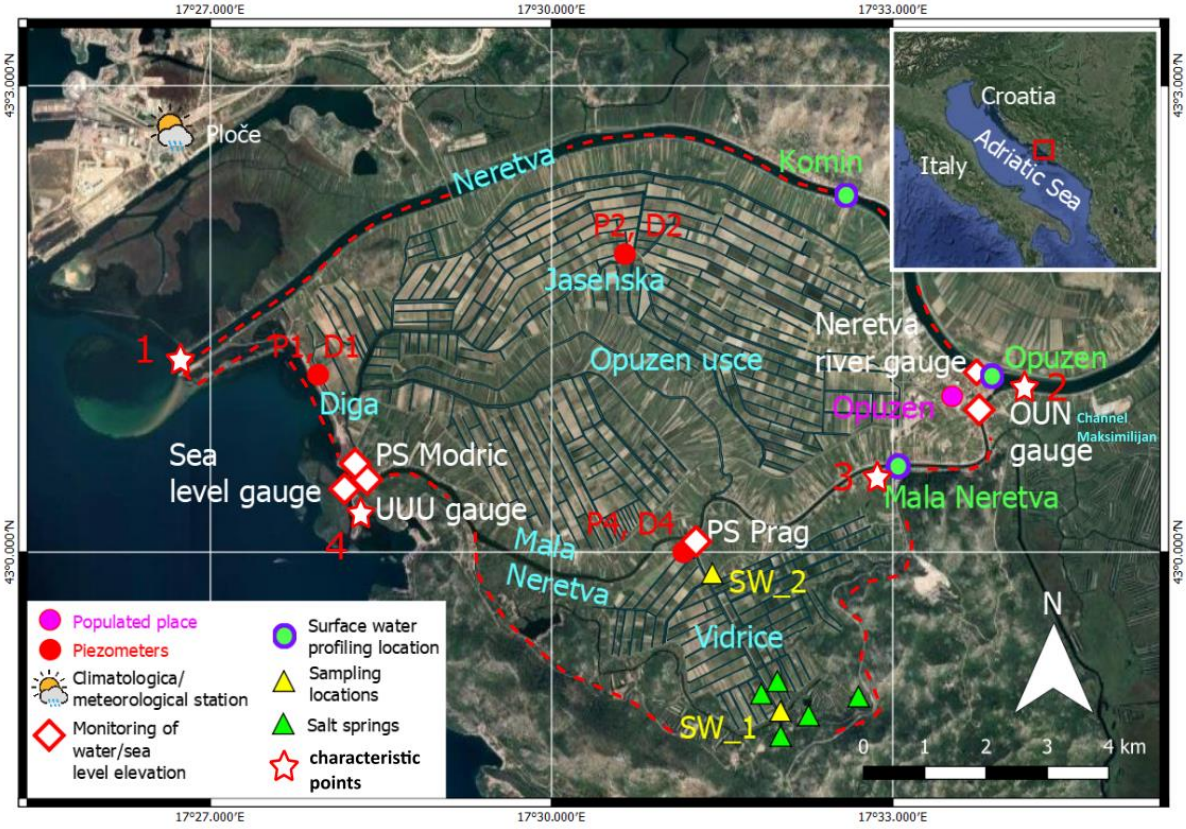

Figure 1. Study area with the definition of monitoring infrastructure locations, melioration system infrastructure, meteorological station, gauges and profiling locations

Meteorological and climatorlogical conditions

Meteorological and climatological conditions along the study area have been provided by data sets observed at the meteorological station Ploče operated by Croatian Hydrometeorological Institute. Ploče station is located about 8 km to the west from the Opuzen town and 2 km to the north west from the Neretva mouth (Figure 1).

During the reference period 2009 - 2019, cumulative annual precipitation ranged from 692,4 to 1768 mm year-1. Through the hydrological year the area of interest is characterized by two main periods, rain season characterizing period from November to April dominantly recognised by frequent precipitation and low air T, and dry season which lasts from May to October with mainly sporadic precipitation occurrence and higher air T. During the period 2010 -2019 rain season cumulative precipitation ranged between 491.2 mm and 1273.8 mm, while dry season cumulative precipitation ranged between 154.9 mm and 670.8 mm (Figure 2).

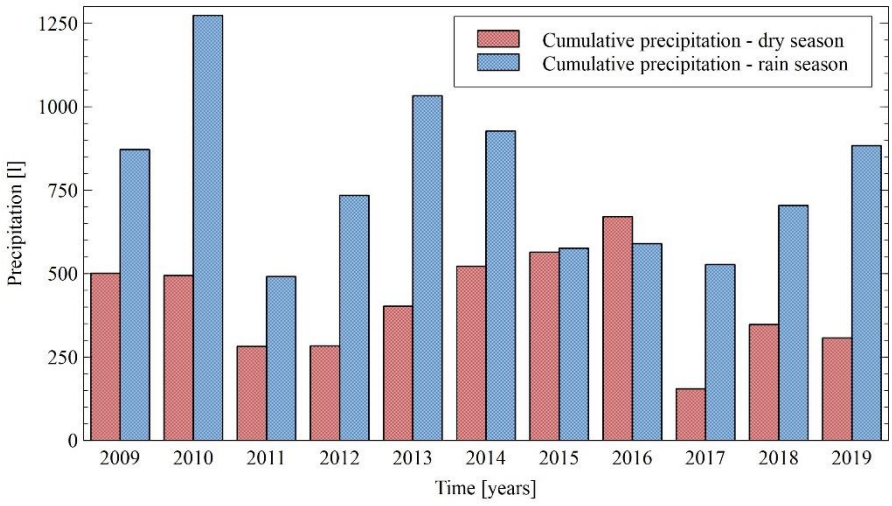

Figure 2. Cumulative precipitation for dry and rain periods observed during 2009 - 2019 at Ploče meteorological station

Geological and hydrogeological settings

The geological definition of the study area has been determined by inspection and

analysis of in situ geotechnical and geophysical investigations performed from 1906s up to date (Elektrosond Zagreb, 1963, 1962; Geofizika Zagreb, 1966, 1962; Geoid-Beroš LTD, 2014; Geokon-Zagreb d.d., 2022, 2013, 2008, 2005; Institute IGH PLC, 2013, 2019). The upper layer representing unconfined aquifer unit consists of fine sands, with local presence of clay and silt. The thickness of clay and silt layers does not exceed 1 m thus representing local heterogeneities. The sand layer is found throughout the study area with a thickness ranging from 1 to 10 m depending on the location (Figure 3). The GWL as found within the sand layer is kept below the sea level with mean annual value of -0.74 m a.s.l. for P1 location as obtained from 2019 observations, -1.93 m a.s.l. for P2 and -1.22 m a.s.l. for P4. Under the sand layer a low conductive layer of clay is found. The clay layer has a thickness of 10-12 m near the city of Opuzen and increases up to 25 m towards the sea. The further extension of this layer under the seabed from the coast to the offshore area is given as about 1400 m (Srzić et al., 2020). Beneath the clay layer a variable depth gravel layer is found. Confinement of this layer is confirmed in the study by Srzic et al. 2020. The depth of this layered roof is reported to be about 20 m in the east and up to 35 m in the west. In the central area of interest and in the northern and southern areas, a conglomerate layer is found at a depth of 40 - 45 m with a thickness of 1 to 3 m. The discontinuity of this layer should be highlighted as this layer was not found in all available boreholes. Beneath the conglomerate layer is an expanse of gravel consisting mostly of fine and medium gravel. The mean annual value of GWL in the confined gravel layer is higher than the mean annual value of SWL (University of Split, 2019). The base of the area is defined with limestone bedrock. The

bedrock was found to be zero on the edge of the Neretva valley, while in the central area, called Crepina, it reaches a depth of 165 m (Institute IGH PLC, 2019).

The determined values of hydraulic conductivity in the confined aquifer range from 7 * 10-4 to 7.5 * 10-3 m s-1 (Srzic et al. 2020) across the entire study area with the effective porosity ranges from 0.15 to 0.25, while the values of specific storage range from 2.87 to 4.97 * 10-6 m-1 (Srzić et al., 2020). Confining geological unit made of clay is characterized by the hydraulic conductivity values ranging from 3.95 * 10-12 to 9.66 * 10-6 m s-1 (Geokon-Zagreb d.d., 2022) On average values of hydraulic conductivity of unconfined aquifer have been determined from 1.15 * 10-4 to – 1.19 * 10-4 (m s-1).

The issue of upstream boundary condition recharge of the upper unconfined aquifer of interest for this study has been shown to be of minor impact to local hydrogeological and salinity conditions as shown in work by Lovrinović et al. 2021., and Lovrinović at al., 2022. Instead, the operation of the melioration system has been shown to overcome local features and effects of precipitation, recharge either lateral inflows from the river Neretva and Mala Neretva.

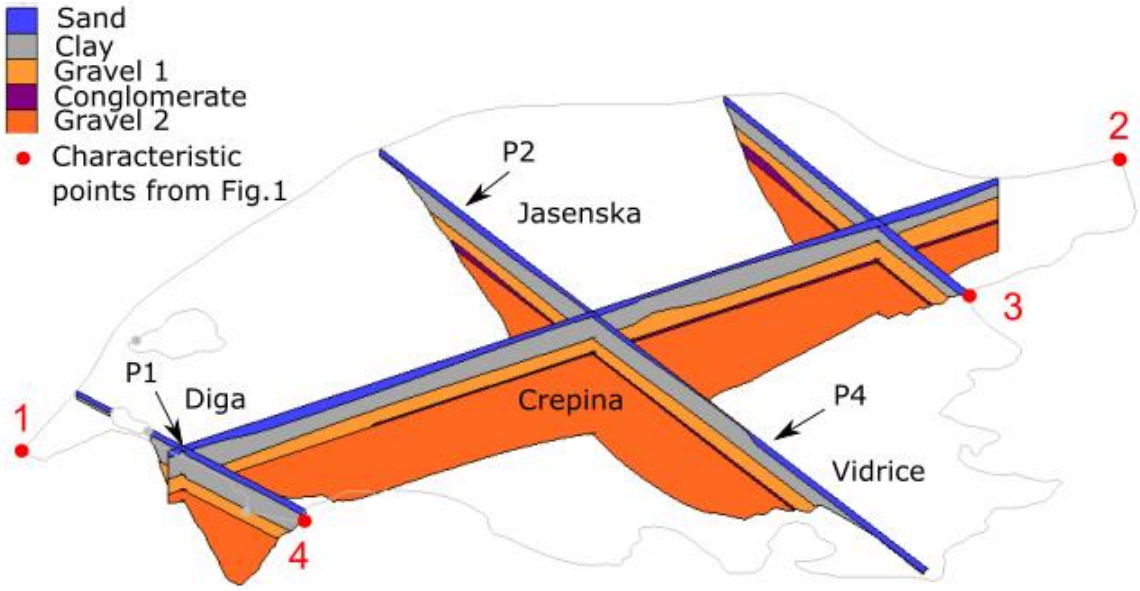

Figure 3. Geological conceptualization of Neretva valley (study area from Figure 1.)

Hydrological conditions

Two main processes, the amount of precipitation over the river basin and the operational regime of the Mostar Hydroelectric Power Plant, located upstream from town Mostar in Bosnia and Herzegovina, define the river Neretva discharge at the study area. From 2009 to 2019 discharge ranged from 40 m3 s-1 to 2092 m3 s-1. The amount of 40 m3 s-1 represents the biological minimum of the Mostar Hydroelectric Power Plant. The Neretva River discharge shows significant seasonal fluctuations. During the dry season (from May to October) the discharge fluctuates between 40 m3 s-1 and 250 m3 s-1 with occasional peaks above 250 m3 s-1, while rain season from November to

April results with discharge values between 200 m3 s-1 and 1700 m3 s-1. Discharge values higher than 1700 m3 s-1 corresponds to specific return periods and are adopted to specified occurrence probabilities (Hrvatske vode, 2014).

Tidal characteristics

The tides in the Adriatic Sea are of mixed diurnal-semidiurnal type (Janeković and Kuzmić, 2005; Srzić et al., 2020), with significant differences in amplitudes between neap and spring tides. The maximum amplitude of the tides in Adriatic Sea ranges from 15 cm in the southern part of the sea to 50 cm in the northern part (Janeković and Kuzmić, 2005). In a study by (Srzić et al., 2020) for the period of August 2015, four dominant tidal constituents were identified within the sea level observations signature, namely O1 and K1 as diurnal constituents and M2 and S2 as semi-diurnal constituents.

Operative regimes

As already explained, Neretva valley is surrounded by rivers Neretva and Mala Neretva. Mala Neretva is a branch of Neretva river separated from the Neretva river by the gates marked as OUN and from the Adriatic Sea by the gates marked as UUU (Figure 1). Mala Neretva system is initially designed to receive excess discharge from the Neretva River to protect the area from flooding. When the discharge of the Neretva river is greater than the capacity of the riverbed, both gates should be opened to evacuate water downstream to the Adriatic Sea. Nowadays, due to anthropogenic interventions in the area of the riverbed Mala Neretva, this system initially planned for flood protection

does not fulfil its original purpose. Instead, it is used as a main source of freshwater during dry season, where water is dispersed from for purpose of irrigation.

To prevent seawater intrusion into Mala Neretva, UUU gates are regulated so the Mala Neretva water elevation is kept higher compared to the SWL. This gradient does not allow sea water cline intrude upstream from the Mala Neretva mouth. Contrary to the UUU, the OUN gates are opened rare, usually only when the water level in Mala Neretva is higher than in Neretva which happens during recession part of Neretva river hydrograph, after the occurrence of peak values. In this way, sea water cline from Neretva riverbed is not allowed to intrude Mala Neretva thus enabling the refreshment of the volume found within the Mala Neretva system. Besides the intermittent refreshment from Neretva riverbed, during dry period Mala Neretva is constantly fed by fresh water from the channel Maksimilijan whose intake is located upstream form Metković town (Figure 1). This enables appropriate amount of fresh water which is used for irrigation of the central part of the area of interest, including Crepina area. Parallel to flood protection and irrigation systems, along the area of interest melioration system is put into operation to keep the groundwater surface elevation below the pedological layer and to enable agricultural production. In order to achieve the groundwater delineation, a system of melioration channels was built whose purpose is to bring water to pumping stations intake basins. The Modric pumping station (PS Modric) has an installed capacity of 19.6 m3 s-1 and is located at the mouth of Mala Neretva. Following Figure 1 it collects the water from Opuzen usce area and transfers it to the Adriatic Sea. The Prag pumping station (PS Prag) has a capacity of 6.5 m3 s-1 (Figure 1) and is used

for delineation of the water table within the Vidrice area by pumping to the river Mala Neretva. Both pumping stations are turned on manually once a day during the night regime. Operation time is controlled by the supervisor of the pumping station and depends on local meteorological and hydrological conditions.

Regardless of the operational time the water level in the pumping station's intake basin is observed at the beginning and end of the working shift, normally at 10 PM and 8 AM, unless additional shifts are required during intensive precipitation events. Water level observations within the intake basins are available prior and post the pumping operation.

C. Methodology

Ground and surface water monitoring system and approaches

In the Lower Neretva Valley, a monitoring system has been installed to observe seawater intrusion parameters in piezometers (Figure 1). These parameters include groundwater level (GWL), electrical conductivity (EC), and temperature (T). At four locations, sea and river surface elevations were observed. Sea level (SWL) was measured near the mouth of river Mala Neretva, whereas river surface elevations (WL) were measured at two locations of Mala Neretva, one downstream from the gate in Opuzen city marked as OUN and the other (UUU) upstream from the gates near the mouth of the river. In the vicinity of the city of Opuzen, the surface elevation of the Neretva river was observed. GWL, EC, and T in an unconfined aquifer were measured

at three locations using piezometers P1, P2, and P4. All piezometers included in the study were drilled 10 meters below ground level with a 12-centimeter-diameter hole. The bottom 9.5 meters of the pipe's screen height have been perforated. Two meters up from the bottom of each piezometer, gauges were positioned. Following the GWL in each shallow piezometer in river Neretva coastal aquifer, only deepest 7-8 m of each piezometer screen is located below the GWL. Deep piezometers consist solely of perforations in a deep, confined aquifer, with total heights of up to 3 m, and are therefore considered as "short screened piezometers". Piezometers with similar perforation heights as used in this study have been successfully used for seawater origin determination (de Oliveira Gomes et al., 2019; Frollini et al., 2022; Pilla and Torrese, 2022; Santucci et al., 2016) and for identification of coastal aquifer external loadings and their influence to groundwater (Fadili et al., 2018; Shin and Hwang, 2020; Zhang et al., 2020).

Surface water monitoring locations are equipped with THALIMEDES OTT gauge with a sampling frequency of 1/hour, measuring range of ±19.999 m, resolution of 0.001 m and accuracy of ±0.002 m. OTT ORPHEUS MINI vented gauge was used in all piezometers to observe GWL and set up to sampling frequency of 1/hour with measuring range from 0 to 40 m and resolution of 0.001 m. A MANTA 2 40+ gauges were also installed in all piezometers to observe groundwater EC and T in piezometers. This gauge has a measuring range of 0 to 100 mS cm-1 with an accuracy of ±1% and 0.0001 mS cm-1 resolution for the EC standardized to 25 °C. The T sensors range is -5 to 50 °C with resolution of 0.01 °C and an accuracy of ±0.1 °C. The timing of all gauges

is synchronized. All gauges and probes used as a setup within the Neretva valley monitoring system are equipped with strain-gauge transducers for measuring the pressure of ground and surface water. The gauges and probes automatically convert pressure readings to a hydrostatic water pressure. In low-lying deltas, it is crucial to measure observe pressure rather than hydraulic head to avoid misinterpretations of groundwater fluxes' direction caused by fluids of variable density (Post et al., 2007). For the purpose of this research, time series obtained from the monitoring network during 2019. Particular focus has been placed to dry and rain periods, specifically August and January. Sea and river gauges provide year-round data on the sea surface and river surface elevation, GWL, EC, and T from borehole P1, and GWL from boreholes P2 and P4. Due to malfunctioning probes, EC and T in boreholes P2 and P4 are available from January to November. The "Nula Trsta" vertical datum is used as a reference for all observed GWL, SWL, and WL values, just as it is for terrain elevation.

In order to gain insight into the vertical stratification of EC and T, six profilings were performed throughout the 2019. Profiling is performed on all piezometers and the Mala Neretva river. They are conducted primarily during the dry season, with the exception of the most recent profile, which was conducted in November and did not include Mala Neretva (Table 1). The SEBA KLL-Q-2 multiparameter probe was used to record GWL and EC T values at various depths. The probe has the following measuring ranges: 0-500 m water column for pressure, -5 to 50 °C for T, and 0-200 mS cm-1 for EC.

Table 1. Locations, dates and time of profilings

		Time and location of profiling			
	Date	P1	P2	P4	MN
1	17.06.2019.	11:30	10:28	09:50	08:00
2	17.07.2019.	12:10	10:57	09:13	08:45
3	22.08.2019.	10:45	09:55	08:15	08:00
4	18.09.2019.	08:30	09:55	11:10	08:35
5	09.10.2019.	11:10	10:15	09:30	08:35
6	25.11.2019.	11:25	12:20	13:25	-

Time series spectrogram and coherence

Observed time series in boreholes, whether the groundwater head or EC, indicate the composition of various aquifer stresses. Each aquifer stress corresponds to a particular frequency or group of frequencies, with amplitude, period, and phase corresponding to each frequency (Dong et al., 2015). Every periodic and aperiodic function in time is decomposed by the Fourier transform into the sum of the sine and cosine functions (Proakis and Manolakis, 2006). Observed signals represent discrete time series, therefore the emphasis of Fourier Transform is on the discrete signals. The formula for Discrete Fourier Transform (DFT) (Cooley et al., 1969) is

$$X_k = \sum_{n=0}^{N-1} x_n e^{\frac{-i2\pi kn}{N}} \qquad k = 0, \dots, N-1 \tag{1}$$

Using Euler's formula Eq. 1 can be written as

$$X_k = \sum_{n=0}^{N-1} x_n \left[cos\left(\frac{2\pi kn}{N}\right) - i \times sin\left(\frac{2\pi kn}{N}\right) \right] \qquad k = 0, \dots, N-1 \tag{2}$$

Or

$$X_k = A_k + iB_k \tag{3}$$

where X_k is the value of the k-th frequency in the frequency bin, k is the number of frequency in the frequency bin, N is the number of samples, x_n is the n-th sample value, and A_k and B_k are complex numbers. The frequency resolution of a plot or frequency bin is defined as the sampling frequency divided by the number of samples. The frequency of the k-th position in the frequency bin is defined as:

$$F_k = n\frac{f_s}{N} \tag{4}$$

where f_s is sampling frequency and n is the sample number. Plotting A_k and B_k in complex plane, magnitude (M) and phase (φ) of each frequency can be calculated.

$$M_k = \sqrt{A_k + B_k} \; ; \quad \varphi_k = tan^{-1}\frac{B_k}{A_k} \tag{5); (6}$$

Typically, DFT results are displayed as amplitude spectral density (ASD) or power spectral density (PSD). Normalizing the DFT results by the number of samples entered in DFT yields an ASD, and the squared value of the ASD's amplitude yields a PSD. The periods and amplitudes of each calculated frequency can be easily deduced from the amplitude spectrum (Fuentes-Arreazola et al., 2018; Srzić et al., 2020; Turnadge et al., 2019).

Stresses on the aquifer can be divided into periodic stresses such as tides, daily changes in atmospheric pressure, daily operating regime of pumping stations and non-periodic stresses, which are usually caused by a change in meteorological conditions or

operating regime. In the case of non-periodic stresses, such as precipitation, the ASD of the aquifer response will have a range of frequencies with different amplitudes to mimic the non-periodic signal (Isermann and Münchhof, 2011) so that a closer look at the time series in the frequency domain is necessary.

Spectrogram and coherence

The coherence model was used to establish a measure of similarity as a function in phase shift between frequencies calculated from observed signals that represent stresses on the aquifer and aquifer response signals. The following is the formula for magnitude square coherence:

$$r(k) = \frac{|G_{XY}(k,\varphi)|^2}{G_{XX}(k)G_{YY}(k)} \quad (7)$$

$G_{XY}(k)$ represents the cross power spectral density (CPSD), whereas $G_{XX}(f)$ and $G_{YY}(f)$ represent the PSD of signals. PSD can also be described as the Fourier transform of the auto-covariance function, while CPSD can be described as the Fourier transform of the cross-covariance function between two signals as a function of phase shift. Coherence values range from 0 to 1, with 1 indicating complete coherence and 0 indicating incoherence.

Since the coherence model does not include information about the amplitude size of the coherence frequencies, it is possible to have significant coherence between both frequencies of interest and noise. The Welch method (Welch, 1967) was used to avoid the interpretation of coherence between noise frequencies and to highlight the

dominant frequencies. First, time series are partitioned into a finite number of smaller time series known as screens, and then the Welch method is applied to each screen. Moving a window over a data set on-screen and calculating the ASD or PSD each time the window is moved is required by the Welch method. The average of all ASDs in a screen is recorded, and all screens are combined to form a spectrogram, which is an image depicting the distribution of all ASDs. The spectrogram provides information about the spectrum's temporal evolution (Pérez-Gómez et al., 2016). To ensure calculation consistency, the Welch method was applied to the spectrogram with the same window shape, size, and overlap points as the coherence model. The results were calculated using modules from the SciPy library, which is integrated with Python 3.7. The coherence models and Welch's method Scipy modules are based on the same study (Welch, 1967).

Observed annual time series were divided into 24 periods (referred to as screens) with 15-day data for each screen (see A. Appendix). The coherence between two time series was calculated for each screen. Using a Tukey window with a shape parameter of 0.25 and a window length of 120 data (5 days), reliable monthly coherence results were determined. The Tukey window was shifted over 110 overlapping data points to generate 24 coherence models for each window. In the results, the mean value of all coherence models was interpreted.

D. Results

To identify and elaborate processes influencing SWI and its impact to groundwater

dynamics within Neretva case study, we separately analyse three locations of interest along the study area. Those three locations correspond to fundamentally different areas respectively: i) Piezometer P1 at Diga area which is dominantly influenced by the SWI, ii) Piezometer P2 located at Jasenska area which is a part of river Neretva left bank area and iii) P4 piezometer which is representative for Vidrice melioration subsystem. The analysis has been performed based on: i) continuous data series of EC, T and GWL, ii) SWL and WL and iii) on borehole profilings of T and EC performed six times during 2019.

Diga area

Figure 4 demonstrates the correspondence of trends of GWL in P1 and SWL. Both trends imply the influence of atmospheric pressure, which can be seen by the increase in the atmospheric pressure and the decrease in GWL and SWL trends, and vice versa. The specific occurrence of such an inverse interdependence of these two variables of interest and the atmospheric pressure is especially evident during significant atmospheric pressure changes during late January, mid and late February, early April and May, mid and late October, and several changes during November and December 2019.

During 2019, PS Modric intake basin water elevation reflects the chainsaw feature which is a consequence of dominantly night operative regime (Figure 4). Turbines are put into operation at the end of the day, usually between 8 and 10 PM, depending on local hydrological and meteorological conditions, while the turnoff is usually scheduled

between 6 and 9 AM. This feature is noticeable by the inspection of spectrogram in Figure 5b, where daily period is observed as present during the whole year of interest. Significant changes in the amplitude of the PS Modric intake basin water surface elevation are present for larger periods during January 2019 when significant decrease in atmospheric pressure and precipitation occurrence are present. The annual mean GWL at P1 equals to 1.09 m beneath than the mean SWL, indicating the presence of active seawater intrusion conditions (Badaruddin et al., 2017, 2015).

In the studies by Lovrinović et al., 2022, 2021 and Srzić et al., 2020, the tidal signal in the SWL characterizing study area is identified of a mixed type, with regular changes in the periods of spring and neap tides (Figure 4). Observed dominant frequencies of GWL in P1 (Figure 5 c)). correspond to the dominant frequencies of the sea level signal (Figure 5 a)). with noticeable decrease in amplitudes due to the attenuation caused by the filtering effect of the aquifer media. The semidiurnal component in the SWL has a larger mean annual amplitude value (0.013 m) compared to diurnal component (0.11 m), while the opposite occurs in the P1 GWL, respectively, the semidiurnal component has a value of 0.028 m and the diurnal has a value of 0.03 m. This is expected since the tidal efficiency is dominantly influenced by the signal period rather than the amplitude. (Erskine, 1991; Jiao and Tang, 1999). Specific yield in the unconfined aquifer can have several orders of magnitude higher values than the storativity in the confined aquifer and therefore the attenuation of sea level oscillations within the unconfined aquifer is larger (Guo et al., 2007; Ratner-Narovlansky et al., 2020) compared to confined aquifer conditions (Srzić et al., 2020). Studies by (Teo et al., 2003; Yeh et al., 2010) have shown

unconfined aquifers in coastal systems can be significantly affected by the SWL fluctuations supporting the similarity with P1 observed GWL.

Deeper inspection of the similarity between the P1 GWL and SWL time series has been derived from the spectrogram analysis as shown in Figure 5a) and c). Hereby, P1 GWL implies the similarity with SWL when analysed in frequency domain. Dominant amplitude spectrum values correspond to mixed tide periods as observed in (Srzić et al., 2020) confirming the dominance of the SWL in the transient definition of P1 GWL. The latter is expected due the fact P1 is located 80 m from the coastline and is therefore directly affected by the SWL variations that couples the effect of the atmospheric pressure and tidal influence. Long-term changes in atmospheric pressure are also visible in the spectrogram of SWL and P1 GWL (Figure 5a) and c)) for the frequencies corresponding to periods higher than daily. Highest amplitude values are present for the periods of January, mid and late February, early April and May, mid and late October, and several changes during November and December (Figure 5 c)). Those periods emphasize the nature of the cause of atmospheric pressure which is explained as a consequence of the air front movement along the pathway over different geographic locations (Dong et al., 2015; Merritt, 2004). The latter is different and should be distinguished from the daily changes in atmospheric pressure, mostly caused by day-night regime of the T change.

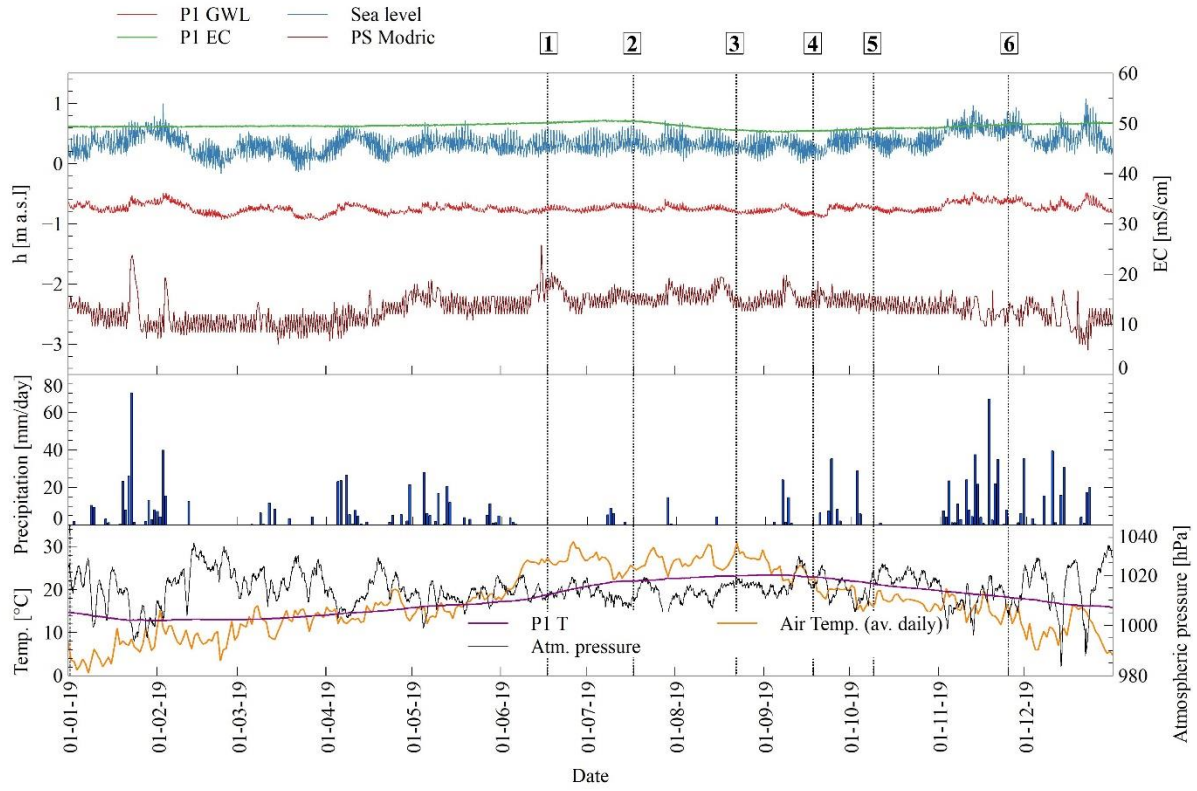

Figure 4. Observed meteorological, hydrological and hydrogeological data, PS Modric intake basin WL, GWL, EC and T for the location P1 and profilings marked with numbers from 1 to 6, for 2019.

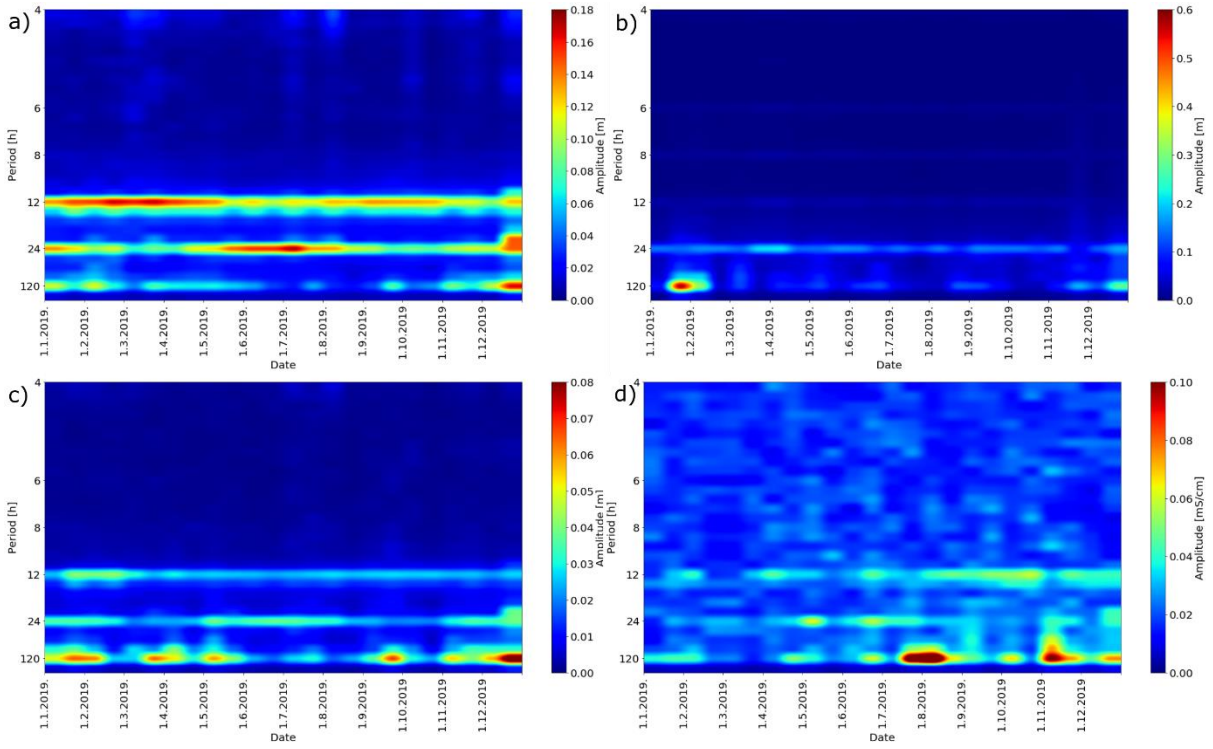

Figure 5. ASD spectrograms representing: a) SWL, b) PS Modric water level, c) P1 GWL and d) P1 EC.

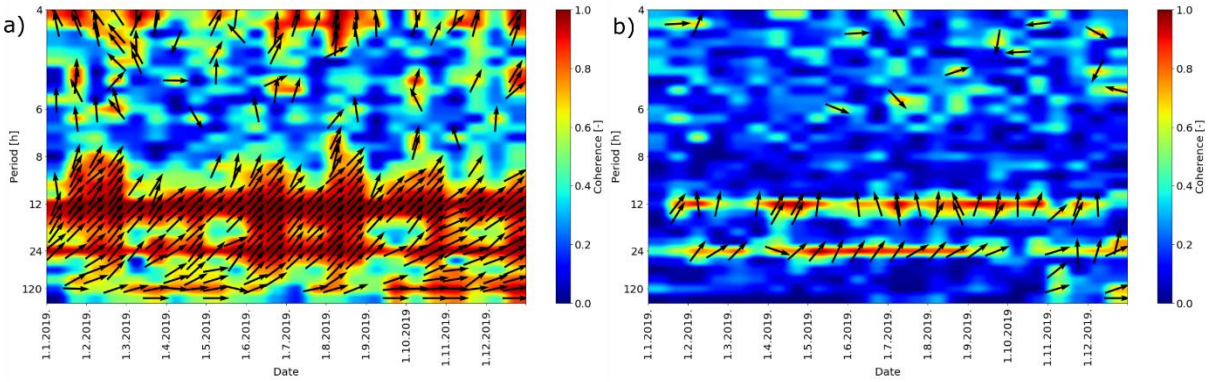

Figure 6. Coherence model between a) SWL and P1 GWL and b) SWL and EC in P1

The values of the coherence model are shown in Figure 6 with the colour bar, where total coherence is marked with red colour and no coherence with blue colour. Arrows indicate the phase in degrees between the same frequency in two signals with coherence determined as 0.6 or higher. An arrow pointing to the right denotes no time lag between two constituents of signals of interest while an arrow pointing to the left means opposite phases of the corresponding constituents. The arrow representation has been shown to be a suitable method for visualising time lags between frequencies in two signals (Briciu, 2019; Zhang et al., 2020). Also, frequencies with periods between 2 and 4 hours were removed from the spectrogram and coherence results because they correspond to noise frequencies (Dong et al., 2015) and to improve the visibility of frequencies of interest. Mean annual coherence values of 0.95 and 0.99 have been determined between diurnal and semidiurnal frequencies corresponding to SWL and GWL in P1, with an annual mean time lag of 2.68 h and 0.77 h standard deviation for the diurnal, and a time lag of 1.58 h and 0.24 h standard deviation for the semidiurnal component. Figure 6a) indicates the SWL and GWL trends occur at the same time implying the cause different than tides.

Following the significant interconnection between SWL and P1 GWL we extend the analysis to EC, assuming the SWL as a driving force controlling the EC in P1. EC in P1 has a relatively constant value varying slightly between 48.16 mS cm^{-1} and 50.7 mS cm^{-1} throughout the year (Figure 4). Coherence inspection between SWL and P1 EC reveals significant values for periods corresponding to the tidal constituents in Figure 6b). Annual mean values of EC time lag relative to SWL corresponds to 2.49 h with coherence

of 0.71 for diurnal constituent. Semidiurnal constituent corresponding time lag equals to 2.58 h with 0.73 coherence value. The standard deviation values of 1.71 h and 0.91 h have been determined for annual time lags of the diurnal and semidiurnal constituents.

Precipitation does not dominate the EC values in P1, compared to SWL influence as can be seen in Figure 4 and 5d) The latter is a consequence of several factors: i) the position of the probe below the transition zone in P1 (Figure 7a)), ii) proximity of the Adriatic Sea, and iii) precipitation occurred at the study area drains towards the melioration channel located 30 m inland from the P1.

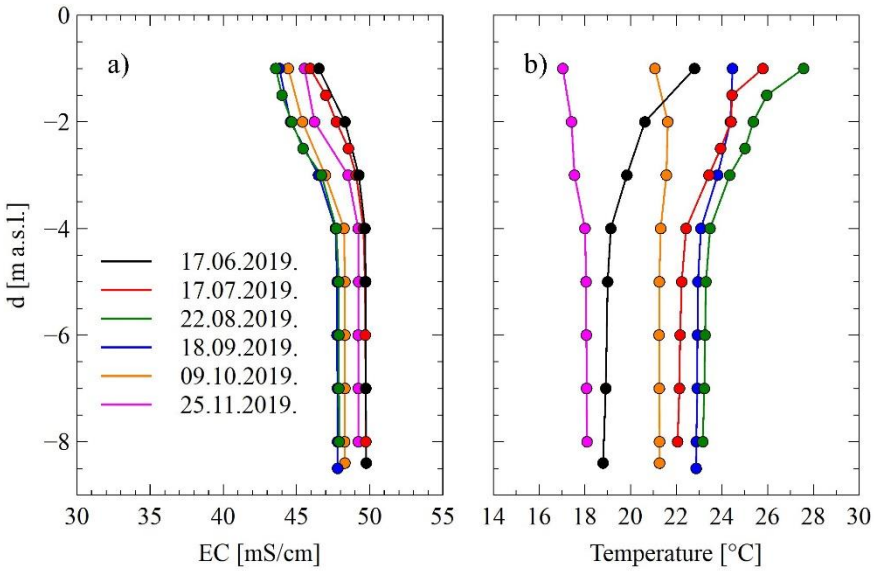

Figure 7. P1 borehole profiles performed six times during 2019: a) EC profiles and b) T profiles

EC borehole profiles (Figure 7a) can be divided into two layers, the first layer (transition zone) from the surface to a depth of -4 m a.s.l. and the second layer from -4 m a.s.l. to

the position of the piezometer probe at -9 m a.s.l.. While EC profiles in unconfined aquifers in the seawater proximity usually show transition from freshwater to seawater in EC profiles (Kim et al., 2008b, 2006; Shin and Hwang, 2020), hereby the transition zone detectable from Figure 7 has a transition zone with a maximum difference between upper and lower values of 4.13 mS cm^{-1}. By coupling the shape of the profiles of EC and the fact the GWL in P1 is found below SWL suggests active seawater intrusion conditions along the Diga area represented by P1 (Badaruddin et al., 2017, 2015). The layer below the transition zone does not show stratification in EC but vary up to maximum 1.96 mS cm^{-1} as observed between the first and fourth profiling.

The T profiles in P1 can be divided vertically into two sub layers, same as for the EC. The first layer up to a depth of 4 m shows vertically varying T, while the second layer below 4 m has relatively constant T (Figure 7b) changing from 18 to 23 °C. Highest observed T in upper layer are observed on July 17th and August 22nd during the peak of the summer season, while highest observed T in deeper layer are recorded on August 22nd and September 18th. This indicates that the upper layer responds faster to changes in air T than the deeper layer which is controlled by the Adriatic Sea T. P1 T increase from 18.80 °C as observed on June 17th to maximum 23.10 °C observed on August 22nd at the piezometer bottom is caused by its proximity to the Adriatic Sea and the influence of SWI. Similar effect but with decreasing trend has been observed during the profiling performed on September 18th, October 9th and finally November 25th when lowest observed T (18 °C) has been observed.

The P1 piezometer is located approximately 80 meters from the coastline and 30 m distance from the melioration channel converging the water towards the PS Modric intake basin. By comparing the mean annual values, the water level in the PS Modric intake basin is determined at 2.74 meters below the sea level, indicating the presence of active seawater intrusion conditions within the area represented by P1. Uniquely, this causes a continuous inflow of seawater into the inland thus transferring the seawater inland. Active SWI results in the salinization of the entire water column and the absence of fresh groundwater discharge to the sea (Badaruddin et al., 2017, 2015). This is confirmed by both the EC and T profiles in P1 (Figure 7a and b), which reveals the presence of seawater in P1. Assumption of the interdependence between P1 T and the Adriatic Sea T has been validated by use of available T time series. Unless the P1 T has been observed by the implemented monitoring system, Adriatic Sea T at the study area has been taken by the available web service (https://seatemperature.info/hr/hrvatska/ploce-temperatura-vode.html) (Figure 8a and b).Although the a-priori dependence is clearly visible from Figure 8a. Figure 8b depicts a cross-correlation model that provides additional confirmation of this. The highest observed cross-correlation coefficient between average daily Adriatic Sea T and average daily P1 T is 0.96 with a time lag corresponding to 6 days implying the P1 T being late for the sea T. Similar finding valid for the EC and piezometric head but with different time scales has been evidenced in the work by Lovrinovic et al., 2022. for the period of August-October 2021. Unless the interdependence of the P1 deeper water column T and the Adriatic Sea T, upper water column T (above -4 m a.s.l.) is dominantly

influenced by the T changes induced by insolation from the air T. Observed cross-correlation coefficient between air T and P1 T corresponds to value of 0.86 with time lag of 18 days (Figure 8b) demonstrating minr influence of air T to control the P1 T compared to sea T influence

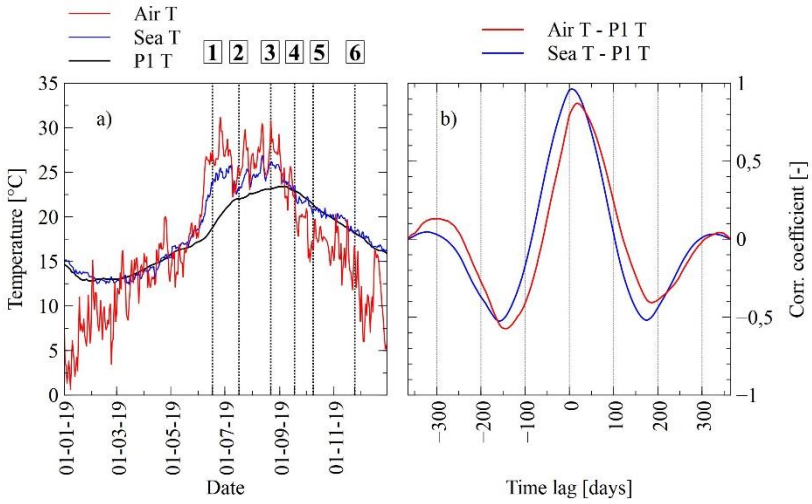

Figure 8. a) Observed average daily T in P1, observed average daily sea T as observed at monitoring station Ploče and observed average daily air T as observed at meteorological station Ploče time series for 2019 and, b) Cross-correlation between air (T) and P1 (T), and sea (T) and P1 (T)

Jasenska area

Inspection of Figure 9 initially emphasize interdependence between river Neretva discharge, PS Modric intake basin surface water elevation and GWL in P2. Following longer precipitation occurrence during rain season, river Neretva discharge is increased reflecting the P2 GWL increase. During the dry season, river Neretva discharge is

observed mainly below 250 m3 s-1 and GWL within the shallow aquifer follows the mean value of the surface water elevation observed in the PS Modric basin thus demonstrating the superiority of PS Modric operation in the definition of the groundwater regime as found along the whole Opuzen usce area and especially Jasenska sub area. It is important to note P2 is located only 75 m away from the channel Jasenska which strengthen the fact about the melioration system operative regime influence to P2 GWL.

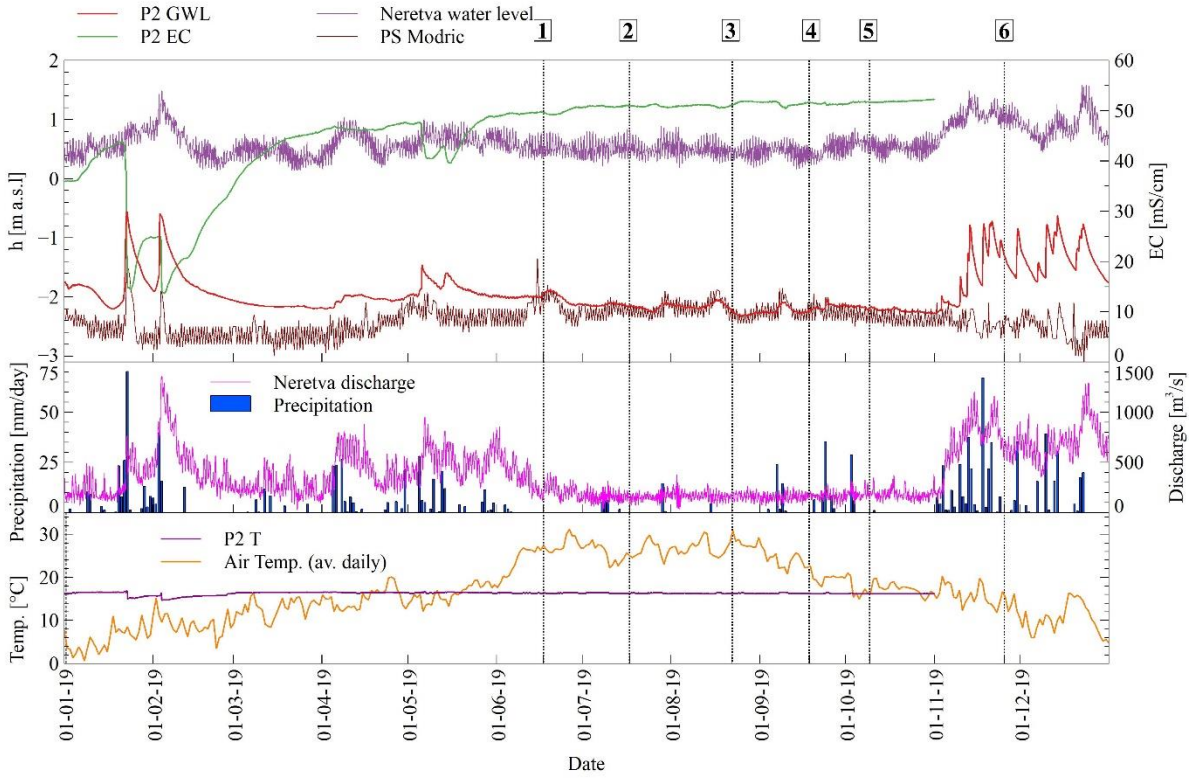

Figure 9. Observed meteorological, hydrological and hydrogeological data, PS Modric intake basin WL, GWL, EC and T for the location P2 and profilings marked with numbers from 1 to 6, for 2019.

The occurrence of precipitation is followed by an increase in P2 GWL (Figure 9 and 10a). In the absence of precipitation during the dry period, the mean GWL in P2 corresponds to the mean water level elevation in PS Modric, emphasizing the influence of PS Modric's operational regime. Daily oscillations in P2 GWL are only detectable via the coherence model between the WL in PS Modric and the GWL in P2 (Figure 11a). These daily oscillations correspond to the PS Modric's night and day operational schedule. Mean coherence values obtained between the PS Modric level and GWL in P2 equals to 0.84 and 0.65 respectively for diurnal and semi-diurnal frequencies during the dry period while precipitation reduces those values of 0.38 and 0.34 respectively (Figure 11a)). This difference distinguishes two periods with different factors controlling the P2 GWL. Unless the rain season causes the change in river Neretva hydrological regime which acts to dominate GWL in Jasenska shallow unconfined aquifer, it is the PS Modric driven melioration system which controls the GWL along the inland of Opuzen usce area during dry season. Inspection of time lags between the PS Modric water elevation induced by precipitation and P2 GWL from the coherence model shown in Figure 11a) reveals the simultaneous change in those variables during precipitation occurrence unless the P2 change driven by the PS Modric operation during dry season is characterised by time lag of 3.23 h for diurnal related frequency.

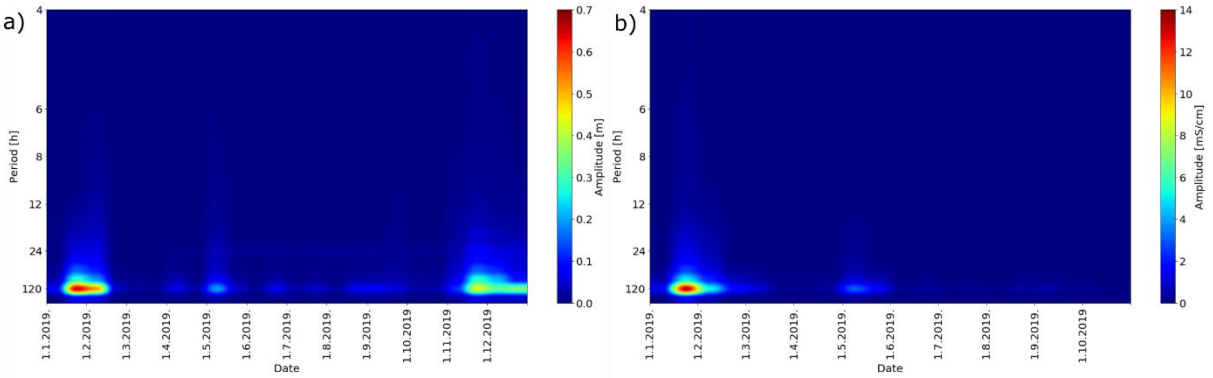

Figure 10. ASD spectrograms representing: a) P2 GWL, b) P2 EC.

Transience of EC as observed at P2 shows different response to precipitation compared to GWL. While the P2 GWL is increased due to the precipitation, EC is reduced. This is especially visible after precipitation of 30 mm day^{-1} or greater. The highest drop in EC value has been observed between January 22nd and February 2nd, when EC decreased by 29.1 mS cm^{-1} to a final value of 13.63 mS cm^{-1} (Figure 9 and 10b)). A similar effect is observed in May after a precipitation of 28 mm day^{-1} but with a less pronounced drop in EC. Although notable amount of precipitation occurred during November and December, the response of EC values in P2 is missed due to probe malfunction during this period. After the precipitation ends, EC in Jasenska area shows exponential recovery feature which reflects slow but significant influence of the external stress controlling the EC rise at the probe depth.

During the dry season, when Neretva discharge falls below 250 m^3 s^{-1}, EC values observed in P2 are usually above 50 mS cm^{-1} which is the evidence of significant volume of seawater affecting the radius of influence of the piezometer. Similar results were presented in the study by (Lovrinović et al., 2021).

Precipitation effects in EC can also be seen in the spectrogram as an increase in drops during late January, early February and early May (Figure 10b). The coherence between PS Modric water level and P2 EC (Figure 11b)) reveals values higher than 0.60 for the frequencies corresponding to the precipitation occurrence during late January, early February, mid July and mid September, as well as for diurnal frequencies during summer. The latter implies the interplay of precipitation and PS Modric operative regime in EC control hereby. The frequencies corresponding to the precipitation occurrence show negative phase of P2 EC relative to PS Modric intake basin water elevation (Figure 11b)), which means the increase of the surface water elevation in the Jasenska channel due to the operating regime of PS Modric causes the decrease in P2 EC and vice versa.

The diurnal components of PS Modric water level and P2 EC possess maximum coherence values of 0.88 and 0.87 respectively during July and August, when the peak of the dry season occurs. Hereby the time lag of the EC relative to the cause of EC change equals to 15 - 17 h.

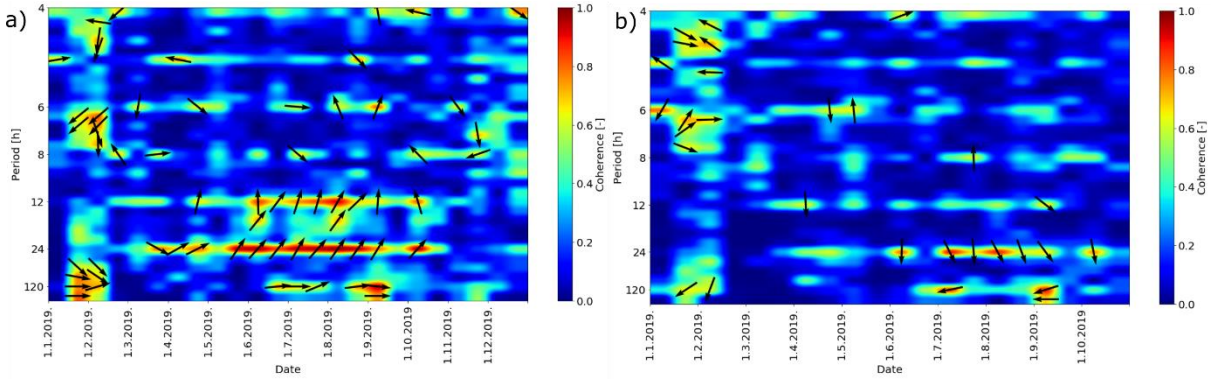

Figure 11. Coherence model between a) PS Modric WL and P2 GWL and b) PS Modric WL and P2 EC.

EC profiles (Figure 12a) were obtained to a depth of -8.3 m a.s.l. (due to the probe location in piezometer) with a maximum value of 45.16 mS cm^{-1} observed above the probe on October 9th (fifth profiling), while the minimum value above the probe was recorded on November 25th (sixth profiling) at 10.49 mS cm^{-1}. The profiling has been performed after long rain period with an average daily river Neretva discharge of 625 m^3 s^{-1} and minor stratification in P2 EC noticed. The profiling performed on June 17th show most significant EC values stratification. This difference is a consequence of the decrease of the Neretva discharge during the transition from rain to dry period, indicating the freshwater from the rainy period is still present in the upper layer of the unconfined aquifer. Four profiles obtained during the dry period show a negligible difference among themselves and a kind of stable groundwater column.

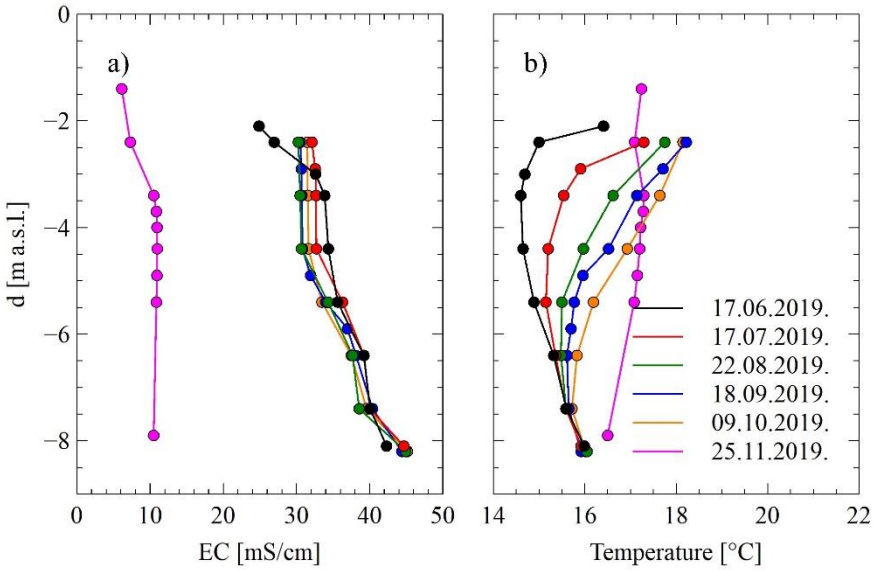

Figure 12. P2 borehole profiles performed six times during 2019: a) EC profiles and b) T profiles

Contrary to EC and GWL, T in P2 shows stability with minor changes except two isolated rainfalls during January 22nd and February 2nd when small decrease in GW T is noticed. For the same reason as mentioned for EC, T data series is not available during November and December. T profiles (Figure 12b) correspond to the recharge type of T profile (Kayane et al., 1985) with constant T at the bottom and pronounced vertical stratification. The main processes of recharge, as seen in Figure 9 and 12 are assumed as infiltration of precipitation into the aquifer and SWI. Surface to ground T may represent T over a time scale, with surface T referring to the effect of daily air T. T observed at final depth may represent the average annual T or the mean T of a longer period as seen in Figure 9.

Vidrice area

P4 GWL has noticeable diurnal oscillations (Figure 13 and 14c)) with an increasing trend during precipitation events. The highest precipitation induced increase has been observed on January 23rd when a precipitation of 70.3 mm day^{-1} caused increase of P4 GWL of 0.87 m. Trends of GWL in P4 and PS Prag intake water elevation caused by precipitation during January, April, May and December coincide as shown in Figure 13, 14b) and c) and 15c).

Diurnal oscillations of P4 GWL does not show transition between spring and neap tide (Figure 13). Instead, regular alternation of one maximum and one minimum daily are observed which corresponds to the operating regime of PS Prag. Tidal efficiency of 0.76 has been identified during August between PS Prag surface water elevation and P4 GWL

representing the dominance of the PS Prag operation in the P4 GWL definition. The coherence model applied to PS Prag water elevation and P4 GWL time series in Figure 15c) confirms corresponding diurnal variations with coherence value 0.99 and no time lag between during whole year since the distance in between is less than 20 m.

Additional inspection of the influences to P4 GWL has been focused to Mala Neretva water elevation represented by UUU. As explained within the chapter 2, Mala Neretva is closed system except during specific circumstances when OUN or UUU gates are opened. Unless no OUN manoeuvre has occurred during 2019, several opening manoeuvres of UUU have been captured based on the insight to UUU time series in Figure 13. Since the gates opening, SWL becomes a boundary condition defining the Mala Neretva water elevation. Periods referring to the UUU opening correspond to late January and early February, early April and May as well as during November and December, as can be seen in Figure 13 and Figure 14a). Due to the connection with the Adriatic Sea, Mala Neretva water elevation shows presence of diurnal and semidiurnal components in its periodicity. The coherence between UUU water level and GWL in P4 has a mean value of 0.7 for the frequency with period of 24 h with varying phase between them (Figure 15a)). This can be explained by the fact both signals are influenced by daily changes in atmospheric pressure in addition to GWL oscillations in P4, where daily oscillations of PS Prag are detectable (Figure 14b and 15c)), thus creating different phases between these two signals.

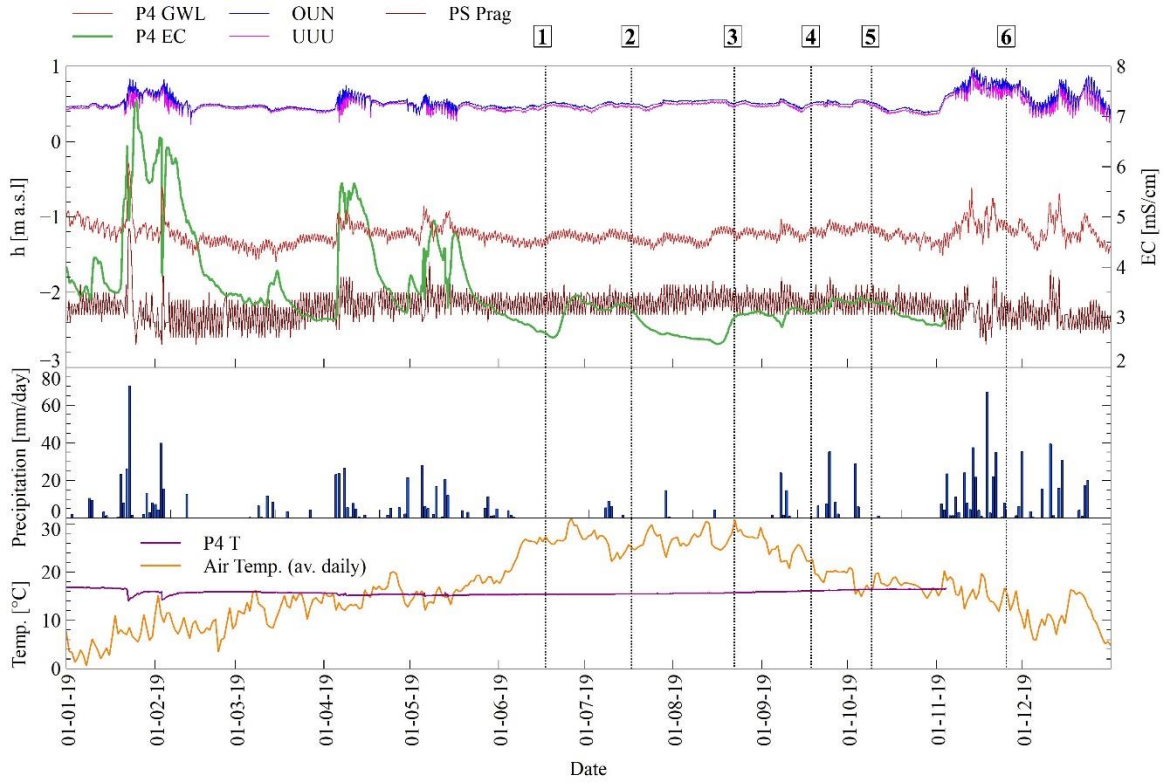

Figure 13. Observed meteorological, hydrological and hydrogeological data, PS Prag intake basin WL, GWL, EC and T for the location P4 and profilings marked with numbers from 1 to 6, for 2019.

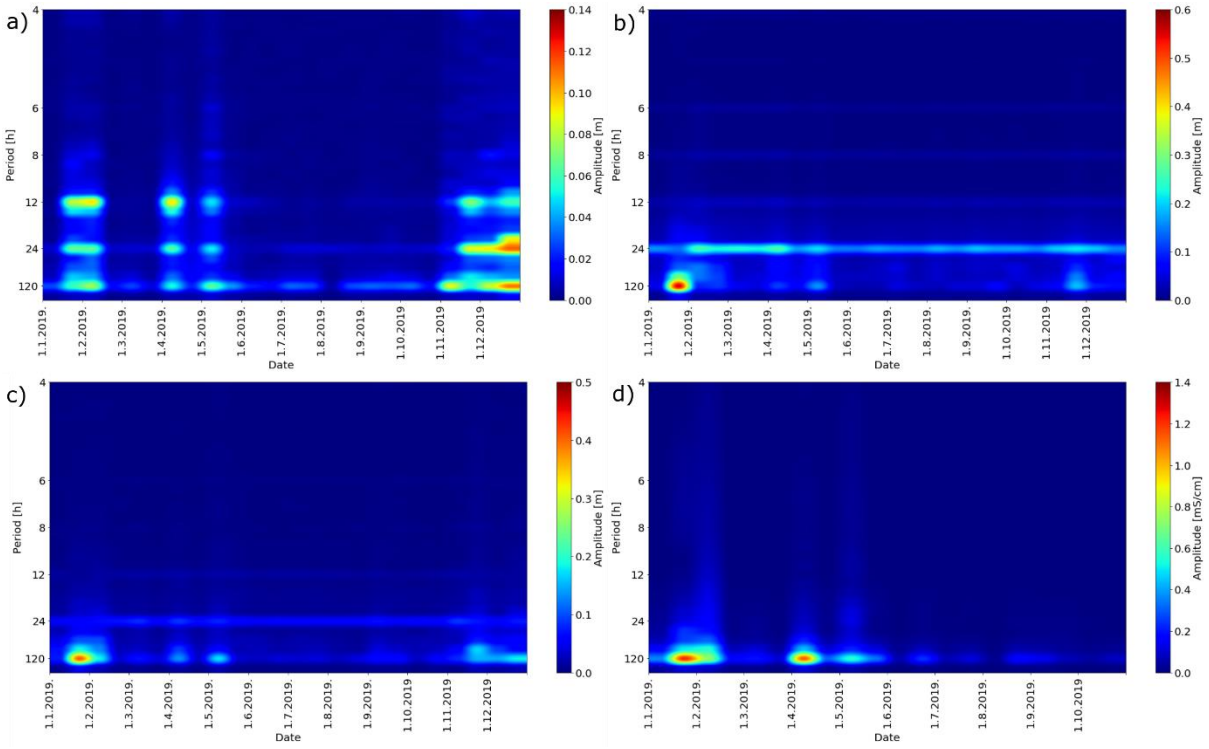

Figure 14. ASD spectrograms representing: a) UUU, b) PS Prag WL, c) P4 GWL and d) P4 EC.

Observed P4 EC values (Figure 13) show that P4 contains mostly brackish water. During the dry period, the EC values are mostly found below 3 mS cm^{-1} at the probe level, while the rain period leads to increase up to 7.31 mS cm^{-1}. From January 20th to January 22nd with on average daily precipitation of 19.1 mm day^{-1}, EC increased from 3.56 mS cm^{-1} to 6.42 mS cm^{-1}. EC reduction from 6.42 mS cm^{-1} to 4.93 mS cm^{-1} has been observed after the precipitation of 70.3 mm day^{-1}. Correspondence in the transient nature of P4 GWL and EC is supported by the spectrograms in Figure 14c) and d). A closer look at those correspondence events shows two phenomena of the behaviour of EC in P4: i)

increase of EC occurs after the precipitation and ii) when the precipitation overcomes approximately 40 mm day^{-1}, EC decreases. Coherence evidences significant correlation between P4 GWL and EC especially during precipitation occurrence (Figure 15b)). Unless precipitation exceed 40 mm day^{-1}, the time lag shows EC change occurs with phase lag equals to half of the period corresponding to the frequency of interest. This means the increase in GWL leads to reduction in EC. The latter is shown to be sensitive to window size used during the coherence analysis performance.

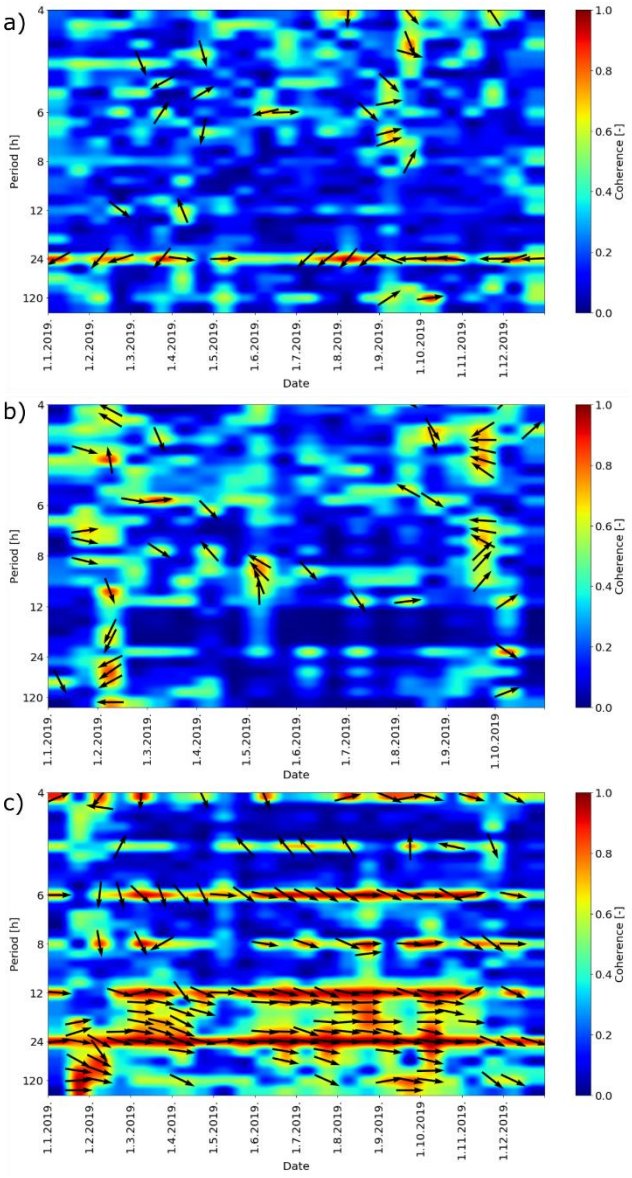

Figure 15. Coherence model between a) UUU level and P4 GWL; b)P4 GWL and EC in P4 and c) PS Prag WL and P4 GWL

The T time series in P4 show similar characteristics to the T observed at P2. The T shows mostly constant values throughout the year, with isolated drops in the T during

precipitation periods. Highest T drops are observed after heavy precipitation in late January and early February. Besides those two events, the T in P4 ranges between 14.95 ºC and 19.11 ºC over the observed period. Inspection of EC and T profiles at P4 and Mala Neretva implies no interdependence (Figure 16a and 16b). EC in P4 fluctuates from 2.40 to 3.15 mS cm^{-1} without the stratification in the unconfined aquifer. Highest T observed during profiling equals to 17.50 °C and has been observed during sixth profiling performed on November 25th. Similar finding has been reported for Jasenska area and P2 piezometer. Previously analysed interdependence between Mala Neretva water elevation and P4 GWL did not show similarity. The inspection of EC profiles emphasizes almost freshwater as found along the Mala Neretva which supports the primary scope of Mala Neretva as a main source of fresh water suitable for irrigation of the area of interest.

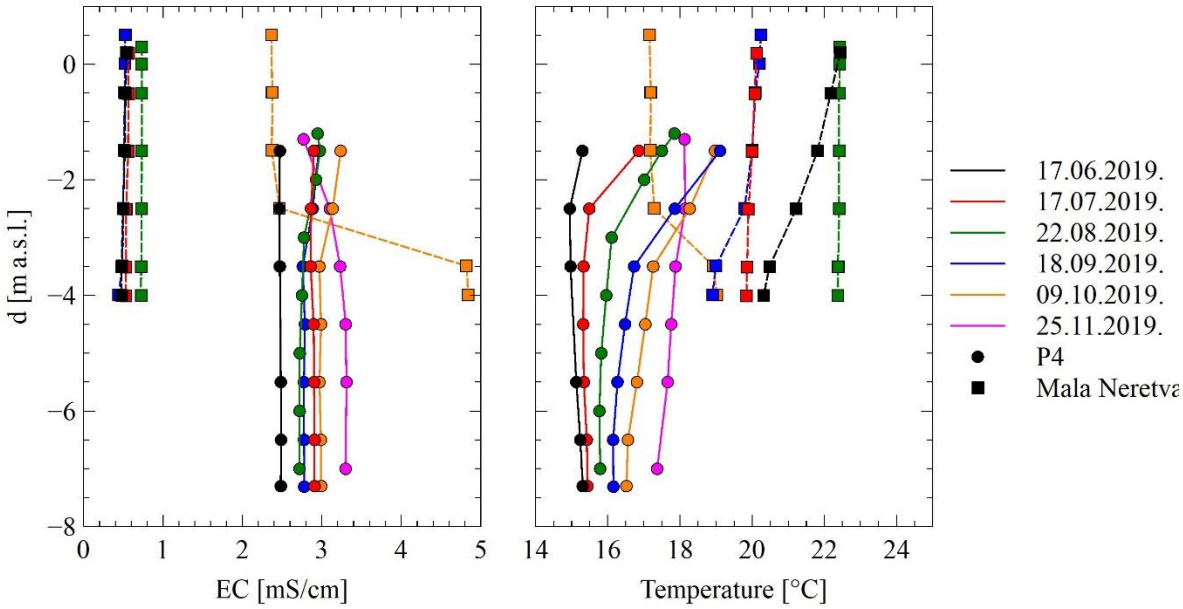

Figure 16. P4 borehole profiles performed six times during 2019: a) EC profiles and b) T profiles

E. Conclusions

This report offers the definition of the external parameters and mechanisms influencing SWI and defining groundwater parameters, respectively GWL, EC and T in river Neretva coastal aquifer system consisted of shallow unconfined aquifer, confining clay layer and confined aquifer. The work relies on three sources: i) time series observed through the implemented monitoring system and ii) profilings performed in-situ, their analysis by application of DFT spectrogram and coherence features analysis and iii) major ion geochemical analysis and indicators. Besides the general conclusion, three different sub areas along the melioration systems Opuzen usce and Vidrice show

fundamentally different conditions and circumstances, below we highlight main findings arose from the presented work:

Diga area representing the embankment delineating Opuzen usce area and the Adriatic Sea represent main corridor for the SWI penetrating Neretva coastal system. Due to the operation of the melioration system, mean groundwater level as found within the shallow unconfined aquifer is found below the mean SWL. This uniquely leads to active SWI conditions resulting in continuous inflow of the seawater to the inland. This 2200 m long barrier between mouth of river Neretva and river Mala Neretva presents a long term corridor for the SWI occurrence into the Neretva coastal system.

Jasenska area GWL and EC regimes are fundamentally different and should be considered separately. Unless the GWL is balanced by river Neretva water elevation and PS Modric operative regime, EC shows changes reflected on a larger temporal scale. Although the changes in GWL are relatively fast, acting as a response to precipitation induced recharge and the regime of Jasenska melioration channel water elevation, EC shows slower response time scales. Although located 1200 m away from the river Neretva left bed, stratification of the salinity within the Neretva river water column induces the lateral SWI to the inland.

GWL in P4 characterizing Vidrice melioration subsystem is shown to be fully determined by the operative regime of PS Prag. Although the GWL regime is driven in this way, EC is driven by the features of brackish upcoming springs found along the southern border of the Vidrice area where karstic hills exceed ground level. Due to the fact the ground level found along this area is strictly beneath the mean sea level and fractured karstic

massive found between the Adriatic Sea and Vidrice area, pathways for the seawater to feed the springs are enabled.

Inspection of main ion geochemical analysis leads towards the conclusion the origin of the salinity of the GW within the shallow unconfined aquifer stems from the SWI. The latter is also supported by the fact of active SWI presence due to the lower GWL relative to mean sea level.

Unless the features of groundwater as found within the shallow unconfined aquifer show sensitivity to external loadings and local circumstances referring to hydrological conditions, tidal features and pumping stations operative regimes, confined aquifer shows stability in EC. The latter is evidenced through similar result obtained in different periods of the hydrological year. Although the piezometric head of the confined aquifer is shown to be dominantly determined by the SWL (Srzić et al., 2020) EC does not behave in the same manner as evidenced from our study.

Transfer of the knowledge gained through the project activities and this deliverable specifically can be accomplished in several key issues and locations along the Croatian coast of the Adriatic sea. Experience from the monitoirng activities could be of great importance due to the significant capacity of the monitoring system to offer reliable data and get insight to processes controling SWI, includig climate change effects. Besides, the transfer of the monitoring experience, expertise in external loadings induced by climate change can also be done to increase the resisitivitiy of other Medditeranean low lying coastal areas to SWI. Potential areas of interest as found alonf the eastern Adriatic coast are: i) islands whose water supply is perfomed by

groundwater exploition fully or partially (e.g.Vis), nature park Vransko Jezero, Vir area, Raša bay, Lim channel area, etc.

F. References

-Khatib, M., Al-Najar, H., 2011. Hydro-Geochemical Characteristics of Groundwater Beneath the Gaza Strip. J. Water Resour. Prot. Vol.3, 341–348. https://doi.org/10.4236/jwarp.2011.35043

Argamasilla, M., Barberá, J.A., Andreo, B., 2017. Factors controlling groundwater salinization and hydrogeochemical processes in coastal aquifers from southern Spain. Sci. Total Environ. 580, 50–68. https://doi.org/https://doi.org/10.1016/j.scitotenv.2016.11.173

Badaruddin, S., Werner, A.D., Morgan, L.K., 2017. Characteristics of active seawater intrusion. J. Hydrol. 551, 632–647. https://doi.org/https://doi.org/10.1016/j.jhydrol.2017.04.031

Badaruddin, S., Werner, A.D., Morgan, L.K., 2015. Water table salinization due to seawater intrusion. Water Resour. Res. 51, 8397–8408. https://doi.org/10.1002/2015WR017098

Bouderbala, A., 2015. Groundwater salinization in semi-arid zones: an example from Nador plain (Tipaza, Algeria). Environ. Earth Sci. 73, 5479–5496. https://doi.org/10.1007/s12665-014-3801-9

Briciu, A.E., 2019. Changes in physical properties of Inland streamwaters induced by

earth and atmospheric tides. Water (Switzerland) 11. https://doi.org/10.3390/w11122533

Carol, E., Perdomo, S., Álvarez, M.D., Tanjal, C., Bouza, P., 2021. Hydrochemical, Isotopic, and Geophysical Studies Applied to the Evaluation of Groundwater Salinization Processes in Quaternary Beach Ridges in a Semiarid Coastal Area of Northern Patagonia, Argentina. Water 13. https://doi.org/10.3390/w13243509

Cooley, J.W., Lewis, P.A.W., Welch, P.D., 1969. The Fast Fourier Transform and Its Applications. IEEE Trans. Educ. 12, 27–34. https://doi.org/10.1109/TE.1969.4320436

Custodio, E., 2010. Coastal aquifers of Europe: an overview. Hydrogeol. J. 18, 269–280. https://doi.org/10.1007/s10040-009-0496-1

Da, C., Carol, E., Kruse, E., Teatini, P., Tosi, L., Da Lio, C., Carol, E., Kruse, E., Teatini, P., Tosi, L., 2015. Saltwater contamination in the managed low-lying farmland of the Venice coast, Italy: An assessment of vulnerability. Sci. Total Environ. 533, 356–369. https://doi.org/10.1016/j.scitotenv.2015.07.013

de Oliveira Gomes, O.V., Marques, E.D., Kütter, V.T., Aires, J.R., Travi, Y., Silva-Filho, E. V., Gomes, O.V.O.O., Marques, E.D., Kütter, V.T., Aires, J.R., Travi, Y., Silva-Filho, E. V., 2019. Origin of salinity and hydrogeochemical features of porous aquifers from northeastern Guanabara Bay, Rio de Janeiro, SE - Brazil. J. Hydrol. Reg. Stud. 22, 100601. https://doi.org/https://doi.org/10.1016/j.ejrh.2019.100601

Delsman, J.R., Hu-a-ng, K.R.M., Vos, P.C., de Louw, P.G.B., Oude Essink, G.H.P., Stuyfzand, P.J., Bierkens, M.F.P., 2014. Paleo-modeling of coastal saltwater intrusion during the Holocene: an application to the Netherlands. Hydrol. Earth Syst. Sci. 18, 3891–3905.

https://doi.org/10.5194/hess-18-3891-2014

Dong, L., Shimada, J., Kagabu, M., Yang, H., 2015. Barometric and tidal-induced aquifer water level fluctuation near the Ariake Sea. Environ. Monit. Assess. 187. https://doi.org/10.1007/s10661-014-4187-6

Elektrosond Zagreb, 1963. Hydrogeological investigation works Opuzen - mouth of Neretva.

Elektrosond Zagreb, 1962. Grain-size distribution curves Opuzen - mouth of Neretva.

Erskine, A.D., 1991. The Effect of Tidal Fluctuation on a Coastal Aquifer in the UK. Groundwater 29, 556–562. https://doi.org/10.1111/j.1745-6584.1991.tb00547.x

Faculty of Civil Engineering; Geodesy and Architecture; University of Split, 2019. Salinity Monitoring at Lower Neretva Area —Report for the year 2019.

Fadili, A., Malaurent, P., Najib, S., Mehdi, K., Riss, J., Makan, A., 2018. Groundwater hydrodynamics and salinity response to oceanic tide in coastal aquifers: case study of Sahel Doukkala, Morocco. Hydrogeol. J. 26, 2459–2473. https://doi.org/10.1007/s10040-018-1812-4

Frollini, E., Parrone, D., Ghergo, S., Masciale, R., Passarella, G., Pennisi, M., Salvadori, M., Preziosi, E., 2022. An Integrated Approach for Investigating the Salinity Evolution in a Mediterranean Coastal Karst Aquifer. Water. https://doi.org/10.3390/w14111725

Fuentes-Arreazola, M.A., Ramírez-Hernández, J., Vázquez-González, R., 2018. Hydrogeological Properties Estimation from Groundwater Level Natural Fluctuations Analysis as a Low-Cost Tool for the Mexicali Valley Aquifer. Water 10. https://doi.org/10.3390/w10050586

Geofizika Zagreb, 1966. Water investigation works at Opuzen – Šetka.

Geofizika Zagreb, 1962. Geophysical investigations /geoelectrical and seismic/ at Opuzen - mouth of Neretva.

Geoid-Beroš LTD, 2014. Piezometer drilling for purpose of groundwater monitoring system.

Geokon-Zagreb d.d., 2022. Field and laboratory research service in the Lower Neretva area for the needs of the Project „Monitoring Sea-water intrusion in coastal aquifers and Testing pilot projects for its mitigation“. Zagreb.

Geokon-Zagreb d.d., 2013. Geotechnical investigation works for siphon below Mala Neretva at the pumping station Prag (Vidrice).

Geokon-Zagreb d.d., 2008. Geotechnical investigation works for irrigation system conceptual design downstream of the Neretva River.

Geokon-Zagreb d.d., 2005. Drilling report of two pairs of piezometers downstream of the Neretva River.

Guo, Q., Li, H., Boufadel, M.C., Xia, Y., Li, G., 2007. Tide-induced groundwater head fluctuation in coastal multi-layered aquifer systems with a submarine outlet-capping. Adv. Water Resour. 30, 1746–1755. https://doi.org/10.1016/j.advwatres.2007.01.003

Hrvatske vode, 2014. Provedbeni plan obrane od poplava branjenog područja sektor f – Južni Jadran branjeno područje 32: područja malih slivova Neretva - Korčula i Dubrovačko primorje i otoci.

Institute IGH PLC, 2019. Monitoring Sea-Water intrusion in coastal aquifers and Testing pilot projects for its mitigation, Geophysical Investigation Report.

Institute IGH PLC, 2013. Geotechnical study for irrigation system Subsystem Opuzen (Phases A and J).

Isermann, R., Münchhof, M., 2011. Spectral Analysis Methods for Periodic and Non-Periodic Signals.

Janeković, I., Kuzmić, M., 2005. Numerical simulation of the Adriatic Sea principal tidal constituents. Ann. Geophys. 23, 3207–3218. https://doi.org/10.5194/angeo-23-3207-2005

Jiao, J., Post, V., 2019. Coastal Hydrogeology. Cambridge University Press, Cambridge. https://doi.org/DOI: 10.1017/9781139344142

Jiao, J.J., Tang, Z., 1999. An analytical solution of groundwater response to tidal fluctuation in a leaky confined aquifer. Water Resour. Res. 35, 747–751. https://doi.org/10.1029/1998WR900075

Kayane, I., Taniguchi, M., Sanjo, K., 1985. Alteration of the groundwater thermal regime caused by advection. Hydrol. Sci. J. 30, 343–360. https://doi.org/10.1080/02626668509490998

Ketabchi, H., Mahmoodzadeh, D., Ataie-Ashtiani, B., Simmons, C.T., 2016. Sea-level rise impacts on seawater intrusion in coastal aquifers: Review and integration. J. Hydrol. 535, 235–255. https://doi.org/https://doi.org/10.1016/j.jhydrol.2016.01.083

Kharroubi, A., Gzam, M., Jedoui, Y., 2012. Anthropogenic and natural effects on the water and sediments qualities of costal lagoons: case of the Boughrara Lagoon (Southeast Tunisia). Environ. Earth Sci. 67, 1061–1067. https://doi.org/10.1007/s12665-012-1551-0

Kim, J.H., Lee, J., Cheong, T.J., Kim, R.H., Koh, D.C., Ryu, J.S., Chang, H.W., 2005. Use of time series analysis for the identification of tidal effect on groundwater in the coastal area of Kimje, Korea. J. Hydrol. 300, 188–198. https://doi.org/10.1016/j.jhydrol.2004.06.004

Kim, K.-Y., Chon, C.-M., Park, K.-H., Park, Y.-S., Woo, N.-C., 2008a. Multi-depth monitoring of electrical conductivity and temperature of groundwater at a multilayered coastal aquifer: Jeju Island, Korea. Hydrol. Process. 22, 3724–3733. https://doi.org/https://doi.org/10.1002/hyp.6976

Kim, K.-Y., Chon, C.-M., Park, K.-H., Park, Y.-S., Woo, N.-C., Kue-Young, K., Chul-Min, C., Ki-Hwa, P., Yun-Seok, P., Nam-Chil, W., 2008b. Multi-depth monitoring of electrical conductivity and temperature of groundwater at a multilayered coastal aquifer: Jeju Island, Korea. Hydrol. Process. 22, 3724–3733. https://doi.org/https://doi.org/10.1002/hyp.6976

Kim, K.-Y.Y., Seong, H., Kim, T., Park, K.-H.H., Woo, N.-C.C., Park, Y.-S.S., Koh, G.-W.W., Park, W.-B.B., 2006. Tidal effects on variations of fresh–saltwater interface and groundwater flow in a multilayered coastal aquifer on a volcanic island (Jeju Island, Korea). J. Hydrol. 330, 525–542. https://doi.org/https://doi.org/10.1016/j.jhydrol.2006.04.022

Krvavica, N., Gotovac, H., Lončar, G., 2021. Salt-wedge dynamics in microtidal Neretva River estuary. Reg. Stud. Mar. Sci. 43, 101713. https://doi.org/https://doi.org/10.1016/j.rsma.2021.101713

Krvavica, N., Ružić, I., 2020. Assessment of sea-level rise impacts on salt-wedge intrusion

in idealized and Neretva River Estuary. Estuar. Coast. Shelf Sci. 234, 106638. https://doi.org/https://doi.org/10.1016/j.ecss.2020.106638

Levanon, E., Yechieli, Y., Gvirtzman, H., Shalev, E., 2017. Tide-induced fluctuations of salinity and groundwater level in unconfined aquifers – Field measurements and numerical model. J. Hydrol. 551, 665–675. https://doi.org/10.1016/j.jhydrol.2016.12.045

Levanon, E., Yechieli, Y., Shalev, E., Friedman, V., Gvirtzman, H., 2013. Reliable monitoring of the transition zone between fresh and saline waters in coastal aquifers. Groundw. Monit. Remediat. 33, 101–110. https://doi.org/10.1111/gwmr.12020

Lovrinović, I., Bergamasco, A., Srzić, V., Cavallina, C., Holjević, D., Donnici, S., Erceg, J., Zaggia, L., Tosi, L., 2021. Groundwater Monitoring Systems to Understand Sea Water Intrusion Dynamics in the Mediterranean: The Neretva Valley and the Southern Venice Coastal Aquifers Case Studies. Water 13. https://doi.org/10.3390/w13040561

Lovrinović, I., Srzić, V., Matić, I., Brkić, M., 2022. Combined Multilevel Monitoring and Wavelet Transform Analysis Approach for the Inspection of Ground and Surface Water Dynamics in Shallow Coastal Aquifer. Water. https://doi.org/10.3390/w14040656

Mastrocicco, M., Colombani, N., 2021. The Issue of Groundwater Salinization in Coastal Areas of the Mediterranean Region: A Review. Water 13. https://doi.org/10.3390/w13010090

Merritt, M.L., 2004. Estimating hydraulic properties of the Floridan Aquifer System by analysis of earth-tide, ocean-tide, and barometric effects, Collier and Hendry Counties, Florida. Water-Resources Investig. Rep. https://doi.org/10.3133/wri034267

Miyakoshi, A., Taniguchi, M., Ide, K., Kagabu, M., Hosono, T., Shimada, J., 2020.

Identification of changes in subsurface temperature and groundwater flow after the 2016 Kumamoto earthquake using long-term well temperature–depth profiles. J. Hydrol. 582, 124530. https://doi.org/10.1016/j.jhydrol.2019.124530

Najib, S., Fadili, A., Mehdi, K., Riss, J., Makan, A., 2017. Contribution of hydrochemical and geoelectrical approaches to investigate salinization process and seawater intrusion in the coastal aquifers of Chaouia, Morocco. J. Contam. Hydrol. 198, 24–36. https://doi.org/10.1016/j.jconhyd.2017.01.003

Oude Essink, G.H.P., van Baaren, E.S., de Louw, P.G.B., 2010. Effects of climate change on coastal groundwater systems: A modeling study in the Netherlands. Water Resour. Res. 46. https://doi.org/https://doi.org/10.1029/2009WR008719

Pérez-Gómez, B., Manzano, F., Alvarez-Fanjul, E., González, C., Cantavella, J. V, Schindelé, F., 2016. Lessons Derived from Two High-Frequency Sea Level Events in the Atlantic: Implications for Coastal Risk Analysis and Tsunami Detection. Front. Mar. Sci. 3. https://doi.org/10.3389/fmars.2016.00206

Pilla, G., Torrese, P., 2022. Hydrochemical-geophysical study of saline paleo-water contamination in alluvial aquifers. Hydrogeol. J. 30, 511–532. https://doi.org/10.1007/s10040-021-02446-5

Post, V., Kooi, H., Simmons, C., 2007. Using hydraulic head measurements in variable-density ground water flow analyses. Ground Water 45, 664–671. https://doi.org/10.1111/j.1745-6584.2007.00339.x

Proakis, J. g., Manolakis, D.G., 2006. Digital Signal Processing, Fourth Edi. ed, Journal of Chemical Information and Modeling. Prentice-Hall, Inc.Division of Simon and Schuster

One Lake Street Upper Saddle River, NJUnited States.

Qin, R., Wu, Y., Xu, Z., Xie, D., Zhang, C., 2013. Assessing the impact of natural and anthropogenic activities on groundwater quality in coastal alluvial aquifers of the lower Liaohe River Plain, NE China. Appl. Geochemistry 31, 142–158. https://doi.org/https://doi.org/10.1016/j.apgeochem.2013.01.001

Racetin, I., Krtalic, A., Srzic, V., Zovko, M., 2020. Characterization of short-term salinity fl uctuations in the Neretva River Delta situated in the southern Adriatic Croatia using Landsat-5 TM. Ecol. Indic. 110, 105924. https://doi.org/10.1016/j.ecolind.2019.105924

Rahi, K.A., Halihan, T., 2013. Identifying aquifer type in fractured rock aquifers using harmonic analysis. GroundWater 51, 76–82. https://doi.org/10.1111/j.1745-6584.2012.00925.x

Ratner-Narovlansky, Y., Weinstein, Y., Yechieli, Y., 2020. Tidal fluctuations in a multi-unit coastal aquifer. J. Hydrol. 580, 124222. https://doi.org/https://doi.org/10.1016/j.jhydrol.2019.124222

Re, V., Zuppi, G.M., 2011. Influence of precipitation and deep saline groundwater on the hydrological systems of Mediterranean coastal plains: a general overview. Hydrol. Sci. J. 56, 966–980. https://doi.org/10.1080/02626667.2011.597355

Romić, D., Castrignanò, A., Romić, M., Buttafuoco, G., Bubalo Kovačić, M., Ondrašek, G., Zovko, M., 2020. Modelling spatial and temporal variability of water quality from different monitoring stations using mixed effects model theory. Sci. Total Environ. 704, 135875. https://doi.org/10.1016/j.scitotenv.2019.135875

Rosenthal, E., Zilberbrand, M., Livshitz, Y., 2007. The hydrochemical evolution of

brackish groundwater in central and northern Sinai (Egypt) and in the western Negev (Israel). J. Hydrol. 337, 294–314. https://doi.org/https://doi.org/10.1016/j.jhydrol.2007.01.042

Saidi, S., Bouri, S., Ben Dhia, H., Anselme, B., 2009. A GIS-based susceptibility indexing method for irrigation and drinking water management planning: Application to Chebba–Mellouleche Aquifer, Tunisia. Agric. Water Manag. 96, 1683–1690. https://doi.org/https://doi.org/10.1016/j.agwat.2009.07.005

Santucci, L., Carol, E., Kruse, E., 2016. Identification of palaeo-seawater intrusion in groundwater using minor ions in a semi-confined aquifer of the Río de la Plata littoral (Argentina). Sci. Total Environ. 566–567, 1640–1648. https://doi.org/https://doi.org/10.1016/j.scitotenv.2016.06.066

Shi, L., Jiao, J.J., 2014. Seawater intrusion and coastal aquifer management in China: a review. Environ. Earth Sci. 72, 2811–2819. https://doi.org/10.1007/s12665-014-3186-9

Shin, J., Hwang, S., 2020. A borehole-based approach for seawater intrusion in heterogeneous coastal aquifers, eastern part of Jeju Island, Korea. Water (Switzerland) 12. https://doi.org/10.3390/w12020609

Sithara, S., Pramada, S.K., Thampi, S.G., 2020. Impact of projected climate change on seawater intrusion on a regional coastal aquifer. J. Earth Syst. Sci. 129. https://doi.org/10.1007/s12040-020-01485-y

Srzić, V., Lovrinović, I., Racetin, I., Pletikosić, F., 2020. Hydrogeological Characterization of Coastal Aquifer on the Basis of Observed Sea Level and Groundwater Level Fluctuations : Neretva Valley Aquifer , Croatia. Water (Switzerland) 12, 348.

https://doi.org/10.3390/w12020348

Teo, H.T., Jeng, D.S., Seymour, B.R., Barry, D.A., Li, L., 2003. A new analytical solution for water table fluctuations in coastal aquifers with sloping beaches. Adv. Water Resour. 26, 1239–1247. https://doi.org/10.1016/j.advwatres.2003.08.004

Turnadge, C., Crosbie, R.S., Barron, O., Rau, G.C., 2019. Comparing Methods of Barometric Efficiency Characterization for Specific Storage Estimation. Groundwater 57, 844–859. https://doi.org/10.1111/gwat.12923

Vallejos, A., Sola, F., Pulido-Bosch, A., 2014. Processes Influencing Groundwater Level and the Freshwater-Saltwater Interface in a Coastal Aquifer. Water Resour. Manag. 29, 679–697. https://doi.org/10.1007/s11269-014-0621-3

Vallejos, A., Sola, F., Yechieli, Y., Pulido-Bosch, A., 2018. Influence of the paleogeographic evolution on the groundwater salinity in a coastal aquifer. Cabo de Gata aquifer, SE Spain. J. Hydrol. 557, 55–66. https://doi.org/https://doi.org/10.1016/j.jhydrol.2017.12.027

Welch, P.D., 1967. The use of fast Fourier transform for the estimation of power spectra: A method based on time averaging over short, modified periodograms. IEEE Trans. Audio Electroacoust. 15, 70–73.

Werner, A.D., Bakker, M., Post, V.E.A., Vandenbohede, A., Lu, C., Ataie-Ashtiani, B., Simmons, C.T., Barry, D.A., 2013. Seawater intrusion processes, investigation and management: Recent advances and future challenges. Adv. Water Resour. 51, 3–26. https://doi.org/10.1016/j.advwatres.2012.03.004

Yang, H., Shimada, J., Shibata, T., Okumura, A., Pinti, D.L., 2020. Freshwater lens

oscillation induced by sea tides and variable rainfall at the uplifted atoll island of Minami-Daito, Japan. Hydrogeol. J. 28, 2105–2114. https://doi.org/10.1007/s10040-020-02185-z

Yechieli, Y., Sivan, O., 2011. The distribution of saline groundwater and its relation to the hydraulic conditions of aquifers and aquitards: examples from Israel. Hydrogeol. J. 19, 71–81. https://doi.org/10.1007/s10040-010-0646-5

Yeh, H.D., Huang, C.S., Chang, Y.C., Jeng, D.S., 2010. An analytical solution for tidal fluctuations in unconfined aquifers with a vertical beach. Water Resour. Res. 46. https://doi.org/10.1029/2009WR008746

Zhang, X., Dong, F., Dai, H., Hu, B.X., Qin, G., Li, D., Lv, X., Dai, Z., Soltanian, M.R., 2020. Influence of lunar semidiurnal tides on groundwater dynamics in estuarine aquifers. Hydrogeol. J. 28, 1419–1429. https://doi.org/10.1007/s10040-020-02136-8

Zovko, M., Romić, D., Colombo, C., Di Iorio, E., Romić, M., Buttafuoco, G., Castrignanò, A., 2018. A geostatistical Vis-NIR spectroscopy index to assess the incipient soil salinization in the Neretva River valley, Croatia. Geoderma 332, 60–72. https://doi.org/https://doi.org/10.1016/j.geoderma.2018.07.005